(2)

NAVAL POSTGRADUATE SCHOOL
Monterey, California

Original contains color plates: All DTIC reproductions will be in black and white

THESIS

TWO - DIMENSIONAL BOUNDARY SURFACES
FOR
AXI - SYMMETRIC EXTERNAL TRANSONIC FLOWS

by

Waleed Isa Al-hashel

March, 1993

Thesis Advisor: Oscar Biblarz

Approved for public release; distribution is unlimited.

DISCLAIMER NOTICE

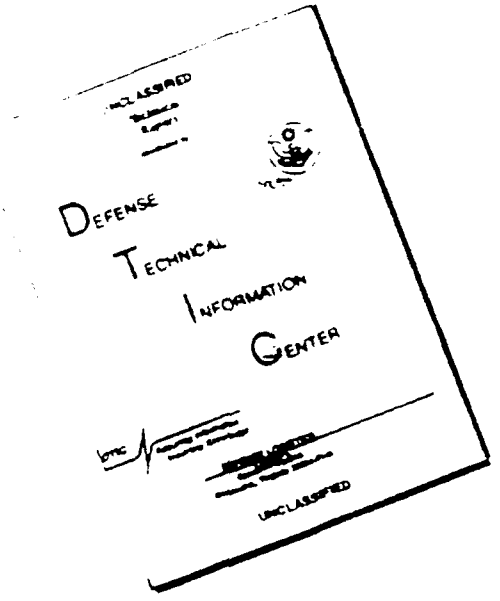

THIS DOCUMENT IS BEST QUALITY AVAILABLE. THE COPY FURNISHED TO DTIC CONTAINED A SIGNIFICANT NUMBER OF PAGES WHICH DO NOT REPRODUCE LEGIBLY.

REPORT DOCUMENTATION PAGE

1a Report Security Classification: Unclassified		1b Restrictive Markings		
2a Security Classification Authority		3 Distribution/Availability of Report		
2b Declassification/Downgrading Schedule		Approved for public release; distribution is unlimited.		
4 Performing Organization Report Number(s)		5 Monitoring Organization Report Number(s)		
6a Name of Performing Organization Naval Postgraduate School	6b Office Symbol *(if applicable)* AA	7a Name of Monitoring Organization Naval Postgraduate School		
6c Address *(city, state, and ZIP code)* Monterey CA 93943-5000		7b Address *(city, state, and ZIP code)* Monterey CA 93943-5000		
8a Name of Funding/Sponsoring Organization	6b Office Symbol *(if applicable)*	9 Procurement Instrument Identification Number		
Address *(city, state, and ZIP code)*		10 Source of Funding Numbers		
		Program Element No	Project No	Task No	Work Unit Accession No

11 Title *(include security classification)* TWO - DIMENSIONAL BOUNDARY SURFACES FOR AXI - SYMMETRIC EXTERNAL TRANSONIC FLOWS.

12 Personal Author(s) Waleed Al-hashel

13a Type of Report	13b Time Covered From To	14 Date of Report *(year, month, day)*	15 Page Count
Master's Thesis		MARCH 1993	70

16 Supplementary Notation The views expressed in this thesis are those of the author and do not reflect the official policy or position of the Department of Defense or the U.S. Government.

17 Cosati Codes			18 Subject Terms *(continue on reverse if necessary and identify by block number)*
Field	Group	Subgroup	TWO - DIMENSIONAL, AXI - SYMMETRIC,EXTERNAL TRANSONIC FLOWS,SMALL PERTURBATION BOUNDARY SURFACES.

19 Abstract *(continue on reverse if necessary and identify by block number)*

Investigation of two-dimensional transonic flows is extended to axisymmetric problems. This is of considerable practical interest, for example, with regard to missiles or aircraft engines which approximate much more closely bodies of revolution than two-dimensional bodies. The main concern with axi-symmetric flows lies not only with the complexity of the governing nonlinear partial differential equation which is mixed of elliptic-hyperbolic type but also with the lack of a general method for accurately solving this type of equation. We solve the nonlinear transonic equation using separation of variables technique, which yields two nonlinear ordinary differential equations. The x-dependence can be integrated numerically, and the solution for the r-dependence can be obtained using the expansion method originated by Van Dyke. This works well with only three terms in the expansion. The sonic solution of these equations is obtained analytically since both equations are simple enough to be integrated for this case ($M_\infty = 1.0$). The small parameter ($1-M_\infty^2$) plays an important role in specifying the shape of the boundary surfaces for external axi-symmetric steady flow of interest for design. A Navier-Stokes solver was used to compute the inviscid flow to confirm our results in the region over the surface where the small perturbations apply.

20 Distribution/Availability of Abstract	21 Abstract Security Classification	
_X_ unclassified/unlimited __ same as report __ DTIC users	Unclassified	
22a Name of Responsible Individual O. Biblarz	22b Telephone *(include Area Code)* (408) 656 - 3096	22c Office Symbol AA/Bi

DD FORM 1473,84 MAR 83 APR edition may be used until exhaustedy d security classification of this page
All other editions are obsolete Unclassified

Approved for public release; distribution is unlimited.

TWO - DIMENSIONAL BOUNDARY SURFACES FOR AXI - SYMMETRIC EXTERNAL TRANSONIC FLOWS

by

Waleed Isa Al-hashel
First Lieutenant, Bahrain Amiri Air Force
B.S., Northrop University, 1987

Submitted in partial fulfillment
of the requirements for the degree of

MASTER OF SCIENCE IN AERONAUTICAL ENGINEERING

from the

NAVAL POSTGRADUATE SCHOOL
March 1993

Author: _____
Waleed Al-hashel

Approved by: _____
Associate Professor O. Biblarz, Thesis Advisor

_____
Associate Professor G. Hobson, Second Reader

_____
Professor D. Collins, Chairman
Department of Aeronautics and Astronautics

ABSTRACT

Investigation of two-dimensional transonic flows is extended to axi-symmetric problems. This is of considerable practical interest, for example, with regard to missiles or aircraft engines which approximate much more closely bodies of revolution than two-dimensional bodies. The main concern with axi-symmetric flows lies not only with the complexity of the governing nonlinear partial differential equation which is mixed of elliptic-hyperbolic type but also with the lack of a general method for accurately solving this type of equation. We solve the nonlinear transonic equation using separation of variables technique, which yields two nonlinear ordinary differential equations. The x-dependence can be integrated numerically, and the solution for the r-dependence can be obtained using the expansion method originated by Van Dyke. This works well with only three terms in the expansion. The sonic solution of these equations is obtained analytically since both equations are simple enough to be integrated for this case (M_∞=1.0). The small parameter ($1-M_\infty^2$) plays an important role in specifying the shape of the boundary surfaces for external axi-symmetric steady flow of interest for design. A Navier-Stokes solver was used to compute the inviscid flow to confirm our results in the region over the surface where the small perturbations apply.

TABLE OF CONTENTS

ACKNOWLEDGEMENTS

I would like to acknowledge the support and guidance of Prof. Oscar Biblarz, thesis advisor, which lead me in preparing this research. I wish also to thank Prof. Garth Hobson for his useful suggestions and comments on the Computational Fluid Dynamics (CFD) portion in this research. Special thanks go to my commanders in the Bahraini Amiri Air Force for giving me the opportunity in getting my graduate education at this school. Finally, I am indebted to my parents for their encouragement and patience during this period.

I. INTRODUCTION

Transonic flow is a classical problem in gas dynamics and yet not many exact solutions are available. The main difficulty lies, of course, in the nonlinearity of the equations and in the boundary conditions.[Ref. 1]

It is of interest to extend two-dimensional flow solutions to axi-symmetric problems, which are more practical for designing bodies of revolution such as missiles or aircraft engines. The goal is to design a shock-free body or surface so we can minimize the penalty of the wave drag that is caused by shock waves. The small perturbation technique may be implemented for simplifying the governing equations and the mathematical procedures for solving the resulting equations in nonlinear flows. This research shows a solution to nonlinear two-dimensional, external flow, over an afterbody axi-symmetric surface. Beginning with the transonic equation for an axi-symmetric body in Chapter II and applying separation of variables gives two nonlinear ordinary differential equations which lead into two exact solutions. One of the nonlinear ordinary differential equation can be integrated numerically, and other one can be solved using the outer expansion method by Van Dyke [Ref. 2]. Chapter III shows the derivation of pressure coefficient and local Mach number for different

surfaces. Supersonic boundary surfaces are obtained implicitly in Chapter IV for M_∞=1.05,1.1, and 1.2 and they are examined by a 3D Navier-Stokes solver, run as an Euler solver for this axi-symmetric problem in Computational Fluid Dynamics (CFD). In addition, the sonic surface is derived analytically in Chapter V. This sonic boundary surface is also examined using 3D Navier-Stokes solver in CFD to verify the results.

II. TRANSONIC EQUATION FOR AXI-SYMMETRIC BODY

The small perturbation, non-linear, axi-symmetric, transonic equation is written as [Ref. 3]

$$(1-M_\infty^2)\,\varphi_{xx} + \frac{1}{r}\frac{\partial}{\partial r}(r\varphi_r) = \varphi_x\varphi_{xx} \qquad (1)$$

Where the non-dimensional axial, x, and radial, r, velocity potentials have been defined as [Ref. 1]

$$\varphi_x \equiv M_\infty^2\,(\gamma+1)\frac{u_x}{U_\infty}, \qquad \varphi_r \equiv M_\infty^2\,(\gamma+1)\frac{u_r}{U_\infty} \qquad (2)$$

where M_∞ is free stream Mach number and γ is ratio of heat capacities.

An exact solution to Equation (1), the transonic equation, can be found from

$$\varphi(x,r) = \varphi^s(x,r) + (1-M_\infty^2)\,x \qquad (3)$$

Which patterned after the two dimensional case given by Biblarz [Ref. 1]. Here φ^s (x,r) is a separable solution for the velocity potential.

The transonic equation in axi-symmetric form, Equation (1), may be separated by letting the potential function $\varphi\ (x,r)$ equal to

$$\varphi\ (x,r) = \xi\ (x)\ \zeta\ (r) + (1-M_\infty^2)\ x \tag{4}$$

Substituting the above function into the transonic equation results in two ordinary, second order, non-linear differential equations

$$\frac{d\xi}{dx}\ \frac{d^2\xi}{dx^2} - \lambda\ \xi = 0 \tag{5}$$

$$\frac{d^2\zeta}{dr^2} + \frac{1}{r}\ \frac{d\zeta}{dr} - \lambda\ \zeta^2 = 0 \tag{6}$$

where λ is the separation constant.

The solution to the first O.D.E.(5) is obtained by multiplying both sides by $d\xi/dx$,

$$\frac{d\xi}{dx}\left(\frac{d\xi}{dx}\ \frac{d^2\xi}{dx^2}\right) - \frac{d\xi}{dx}\ (\lambda\ \xi) = o \tag{7}$$

or

$$\frac{d}{dx}\left[\ \frac{1}{3}\left(\frac{d\xi}{dx}\right)^3 - \frac{\lambda}{2}\ \xi^2\ \right] = 0 \tag{8}$$

Thus

$$\frac{d\xi}{dx} = \left(\frac{3}{2}\lambda\xi^2 + \alpha \right)^{\frac{1}{3}} \tag{9}$$

Rearranging

$$dx = \frac{d\xi}{\left(\frac{3}{2}\lambda\xi^2 + \alpha \right)^{\frac{1}{3}}} \tag{10}$$

and integrating

$$x - x_0 = \int \frac{d\xi}{\left(\frac{3}{2}\lambda\xi^2 + \alpha \right)^{\frac{1}{3}}} \tag{11}$$

where α and x_o are integration constants.

The solution to the second non-linear O.D.E.(6), is obtained by an outer expansion method. [Ref. 2]

$$\zeta(r) = \frac{4}{\lambda r^2} + (1-M_\infty^2) f_1(r) + (1-M_\infty^2)^2 f_2(r) + \ldots \tag{12}$$

Where $(1-M_\infty^2)$ represents a small parameter and the first term is the purely sonic solution.

By taking first and second derivatives and substituting them into the original 2nd order, non-linear, O.D.E.(6), the solution becomes

$$\zeta(r) = \frac{1}{\lambda r^2}\left[4 + |1-M_\infty^2| a\lambda r^{(\sqrt{8}+2)} + \frac{(1-M_\infty^2)^2}{28+8\sqrt{8}} a^2\lambda^2 r^{2(\sqrt{8}+2)} + \ldots\right] \quad (13)$$

where a is constant.

Equations 11 and 13 are solutions to the differential equations 5 and 6. Boundary conditions are needed to determine the constants α, C_1, a, and λ.

The constants C_1, a, and λ can be shown to be related by the expression [Ref.1]

$$\left(\frac{C_1}{\lambda}\right)\frac{a^{1.2426}}{\lambda^{0.7574}} = 1.08x10^{-2} \quad (14)$$

and

$$\alpha = \pm C_1 |1-M_\infty^2|^{1.7574} \quad (15)$$

The positive sign above is for $M_\infty \geq 1.0$ and the negative sign is for $M_\infty < 1.0$.

Upon inserting Eqn.(15) into Eqn.(11), we have

$$x-x_0=\int \frac{d\xi}{\left[\frac{3}{2}\lambda\,\xi^2+C_1\left|1-M_\infty^2\right|^{1.7574}\right]^{\frac{1}{3}}} \tag{16}$$

Factoring out C_1, we obtain

$$x-x_0=C_1^{-\frac{1}{3}}\int \frac{d\xi}{\left[\frac{3}{2}\lambda\,\frac{\xi^2}{C_1}+\left|1-M_\infty^2\right|^{1.7574}\right]^{\frac{1}{3}}} \tag{17}$$

Introducing new variables

$$\xi \equiv \xi\left(\frac{3\lambda}{2C_1}\right)^{\frac{1}{2}} \tag{18}$$

$$\bar{r}^{(\sqrt{8}+2)} \equiv r^{(\sqrt{8}+2)}\lambda\, a \tag{19}$$

Equations (17) and (13) become

$$x-x_0=C_1^{\frac{1}{6}}\left(\frac{3\lambda}{2}\right)^{-\frac{1}{2}}\int \frac{d\xi}{\left[\xi^2+\left|1-M_\infty^2\right|^{1.7574}\right]^{\frac{1}{3}}} \tag{20}$$

$$\zeta = \frac{(a\lambda)^{0.4142}}{\lambda \tilde{f}^2}\left[4 + \left|1-M_\infty^2\right| \tilde{f}^{(\sqrt{8}+2)} + \frac{(1-M_\infty^2)^2}{50.63}\tilde{f}^{2(\sqrt{8}+2)}\right] \tag{21}$$

Finally, defining two new variables

$$\tilde{X} \equiv C_1^{-\frac{1}{6}}\, x \left(\frac{3\lambda}{2}\right)^{\frac{1}{2}} \tag{22}$$

$$\zeta \equiv \frac{\zeta\, \lambda}{(a\ \lambda)^{0.4142}} \tag{23}$$

Equations 20 and 21 become

$$\tilde{X} = \int \frac{d\xi}{\left[\xi^2 + \left|1-M_\infty^2\right|^{1.7574}\right]^{\frac{1}{3}}} \tag{24}$$

where $x_0=0$.

$$\zeta = \frac{1}{\tilde{f}^2}\left[4 + \left|1-M_\infty^2\right| \tilde{f}^{(\sqrt{8}+2)} + \frac{(1-M_\infty^2)^2}{50.63}\tilde{f}^{2(\sqrt{8}+2)}\right] \tag{25}$$

Equation (24) will be numerically integrated and plotted in Fig. (1) as $\xi(\tilde{X})$ vs. $\tilde{X}$, and Equation (25) will be evaluated and plotted in Fig.(2) as $\zeta(\tilde{f})$ vs. $\tilde{f}$ for M_∞= 1.05, 1.1, 1.2. These results will be used later to obtain transonic surfaces with their corresponding C_p and local Mach number

profiles. In Fig.(2), Equation (25) is plotted up to its minimum value with increasing $\tilde{r}$. Thereafter, a constant value is patched in to the right of the + mark. This is done because of the need to keep ζ constant reflecting the necessary behavior of the function for range $\tilde{r}$ [Ref.1].

III. PRESSURE COEFFICIENT AND LOCAL MACH NUMBER

The pressure coefficient for a flow with small perturbations is given by [Ref. 4]

$$C_p = -\left[\frac{2u_x}{U_\infty} + (1-M_\infty^2) \left(\frac{u_x}{U_\infty}\right)^2 + \left(\frac{u_r}{U_\infty}\right)^2 \right] \tag{26}$$

The linearized pressure approximation for axi-symmetric flow is

$$C_p = \frac{-2\ u_x}{U_\infty} \tag{27}$$

Recall the axial velocity potential, Equation (2), Chapter II,

$$\varphi_x = M_\infty^2\ (\gamma+1)\ \frac{u_x}{U_\infty} \tag{28}$$

thus

$$\frac{u_x}{U_\infty} = \frac{\varphi_x}{M_\infty^2\ (\gamma+1)} \tag{29}$$

substitute Equation (29) into Equation (27), yields

$$C_p = \frac{-2\ \varphi_x}{M_\infty^2\ (\gamma+1)} \tag{30}$$

We need to take the derivative of the potential function with respect to x in equation (4).

$$\varphi_x = \zeta\ \frac{d\xi}{dx} + (1 - M_\infty^2) \tag{31}$$

Rewriting equation (9) with the constant α inserted becomes

$$\frac{d\xi}{dx} = \left[\frac{3\lambda}{2}\ \xi^2 + C_1\ |\ (1-M_\infty^2)\ |^{1.7574}\right]^{\frac{1}{3}} \tag{32}$$

Recall Equation (18)

$$\xi = \xi \left(\frac{3\lambda}{2C_1}\right)^{\frac{1}{2}} \tag{33}$$

Inserting Eqn.(33) into Eqn.(32) and factoring C_1 out, yields

$$\frac{d\xi}{dx} = C_1^{\frac{1}{3}} \left[\ \xi^2 + |\ (1-M_\infty^2)\ |^{1.7574}\ \right]^{\frac{1}{3}} \tag{34}$$

Recall Equation (23) and rearrange

$$\zeta = \frac{(a\,\lambda)^{0.4142}}{\lambda}\,\zeta \tag{35}$$

Rewriting Equation (31) the potential function as

$$\varphi_x = \frac{(a\lambda)^{0.4142}}{\lambda}\,\zeta\, C_1^{\frac{1}{3}}\left[\,\xi^2+\left|(1-M_\infty^2)\right|^{1.7574}\right]^{\frac{1}{3}}+(1-M_\infty^2) \tag{36}$$

Thus

$$\varphi_x = \frac{a^{0.4142}C_1^{\frac{1}{3}}}{\lambda^{0.5858}}\,\zeta\left[\,\xi^2+\left|(1-M_\infty^2)\right|^{1.7574}\right]^{\frac{1}{3}}+(1-M_\infty^2) \tag{37}$$

Recall Equation (14) Chapter II

$$\left(\frac{C_1}{\lambda}\right)\frac{a^{1.2426}}{\lambda^{0.7574}} = 1.08x10^{-2} \tag{38}$$

then finally Equation (37) becomes

$$\varphi_x = 0.2208\,\zeta\left[\,\xi^2+\left|(1-M_\infty^2)\right|^{1.7574}\right]^{\frac{1}{3}}+(1-M_\infty^2) \tag{39}$$

Rewriting the coefficient of pressure

$$C_p=\frac{-2}{M_\infty^2(\gamma+1)}\left[0.2208\,\zeta\left[\xi^2+\left|(1-M_\infty^2)\right|^{1.7574}\right]^{\frac{1}{3}}+(1-M_\infty^2)\right] \tag{40}$$

The previous expression for C_p will be used further in determining the local Mach number.

The perturbation velocities are assumed to be vary small compared to the undisturbed uniform velocity U_∞. [Ref. 5]

Hence at a point near the body, the velocity vector $\vec{V}$ for 2-D flow is given by

$$\vec{V} = i(U_\infty + u_x) + j\, u_r \tag{41}$$

We can obtain the local Mach number M in terms of the perturbation velocities and the local speed of sound c as

$$M^2 = \frac{|\vec{V}|^2}{C^2} = \frac{(U_\infty + u_x)^2 + u_r^2}{C^2} \tag{42}$$

Neglecting the higher order ratios of the free stream to perturbation velocities, since they are considerably smaller than unity, we have

$$M^2 = \frac{U_\infty^2 \left(1 + \frac{2u_x}{U_\infty}\right)}{C^2} \tag{43}$$

The ratio of the local speed of sound to the undisturbed uniform speed of sound becomes

$$\frac{c^2}{c_\infty^2} = \frac{T}{T_\infty} \tag{44}$$

or

$$\frac{c^2}{c_\infty^2} = \frac{T_o/T_\infty}{T_o/T} \tag{45}$$

Where T_o is the stagnation temperature.

We can write temperature ratios as functions of Mach numbers as

$$\frac{c^2}{c_\infty^2} = \frac{1 + \frac{(\gamma-1)}{2}M_\infty^2}{1 + \frac{(\gamma-1)}{2}M^2} \tag{46}$$

Substituting Equation (45) into Equation (46) and rearrange, we have

$$M^2 = M_\infty^2 \frac{\left(1+\frac{2u_x}{U_\infty}\right)\left(1+\frac{(\gamma-1)}{2}M^2\right)}{\left(1+\frac{\gamma-1}{2}M_\infty^2\right)} \tag{47}$$

from Equation (27)

$$C_p = \frac{-2\ u_x}{U_\infty} \tag{48}$$

Rearranging and solving for local Mach number

$$M^2 = \frac{M_\infty^2\ (1-C_p)}{1 + \frac{\gamma-1}{2} M_\infty^2\ C_p} \tag{49}$$

This equation will be used to show the local Mach number for each surface at M_∞ = 1.05, 1.1 and 1.2 [Ref. 6].

IV. SUPERSONIC BOUNDARY SURFACES

The boundary conditions which need to be applied require that the gradient of φ vanish far ahead of the body and that the flow be tangential to the surface [Ref. 7]. In terms of perturbation velocities the boundary conditions become

$$\left(\frac{dr}{dx}\right)_{surface} = \frac{u_r}{U_\infty} \tag{50}$$

Recall the modified velocity perturbation potential Eqn.(2)

$$\varphi_r = M_\infty^2 \ (\gamma + 1) \frac{u_r}{U_\infty} \tag{51}$$

then, we have

$$\frac{u_r}{U_\infty} = \frac{\varphi_r}{M_\infty^2 \ (\gamma+1)} \tag{52}$$

by substituting Equation (52) into Equation (50), we obtain

$$\left(\frac{dr}{dx}\right) = \frac{\varphi_r}{M_\infty^2 \ (\gamma+1)} \tag{53}$$

By differentiating Equation (4) with respect to r gives

$$\varphi_r = \xi \frac{d\zeta}{dr} \tag{54}$$

Recalling Eqn.(18) and substituting Eqn.(21) into Eqn.(23), and taking the derivative with respect to $\tilde{r}$, the above equation becomes

$$\varphi_r = 0.0848 \ \xi \frac{d\zeta}{d\tilde{r}} \tag{55}$$

Substituting Equation (55) and (13) into equation (53), we have

$$\left(\frac{dr}{dx}\right) = \frac{0.0848}{M_\infty^2(\gamma+1)} \xi \left[\frac{-8}{\tilde{r}^3} + 2.8284 \ |1-M_\infty^2| \ \tilde{r}^{1.8284} + 0.1512 \ (1-M_\infty^2)^2 \ \tilde{r}^{6.657}\right] \tag{56}$$

It can be noticed here that ξ and ζ are given implicitly as function of $\tilde{x}$ and $\tilde{r}$ respectively.

From Eqns.(19) and (22), we can rearrange Equation (56) as

$$\frac{d\tilde{r}}{d\tilde{x}} = \frac{3.26x10^{-2}}{M_\infty^2(\gamma+1)} \xi \left[\frac{-8}{\tilde{r}^3} + 2.8284 \ |1-M_\infty^2| \ \tilde{r}^{1.8284} + 0.1512 \ (1-M_\infty^2)^2 \ \tilde{r}^{6.657}\right] \tag{57}$$

Further arrangment of the previous equation yields

$$\frac{d\tilde{r}}{\left[\frac{8}{\tilde{r}^3}-2.8284\left|1-M_\infty^2\right|\tilde{r}^{1.8284}-0.1512\left(1-M_\infty^2\right)^2\tilde{r}^{6.657}\right]} = \frac{-3.26x10^{-2}}{M_\infty^2(\gamma+1)}\,\xi\,d\tilde{x} \tag{58}$$

Now, we can compute the exact boundary surfaces out of the equation above. Starting with the left hand side of the equation

$$Z(\tilde{r}) = \frac{\tilde{r}^3}{\left[8-2.8284\left|1-M_\infty^2\right|\tilde{r}^{4.8284}-0.1512\left(1-M_\infty^2\right)^2\tilde{r}^{9.657}\right]} \tag{59}$$

By defining equation (59) we can plot $Z(\tilde{r})$ vs. $\tilde{r}$ in Fig. (3) for M_∞ = 1.05, 1.1, and 1.2.

The minimum values of $\tilde{r}_o$ for different Mach numbers can be expressed as $\tilde{r}_o = \tilde{r}_o(M_\infty)$ which has been found to be [Ref. 1]

$$\tilde{r}_o = \frac{1.2074}{\left|1-M_\infty^2\right|^{0.2071}} \tag{60}$$

Fig. (4) represents $\tilde{r}_o$ vs. M_∞ and shows a symmetry close to M_∞=1.0 where $\tilde{r}_o=\infty$. So for our purpose to represent the condition sufficiently close to M_∞ = 1.0, we will choose a finite value of $\tilde{r}_o$ (perhaps as 4.0).

Defining the right hand side of Equation (58) as

$$K(\tilde{x}) = \frac{-3.26x10^{-2}}{M_\infty^2(\gamma+1)} \int_0^{\tilde{x}} \xi \, d\tilde{x} \qquad (61)$$

taking the derivative of Equation (24) and substitute it into Equation (61), yields

$$K(\tilde{x}) = \frac{-3.26x10^{-2}}{M_\infty^2(\gamma+1)} \int_0^{\xi} \frac{\xi \, d\xi}{[\xi^2+|1-M_\infty^2|^{1.7574}]^{\frac{1}{3}}} \qquad (62)$$

integrating by parts, we obtain

$$K(\tilde{x}) = \frac{-2.45x10^{-2}}{(\gamma+1)M_\infty^2}\left[\left(\xi^2-|1-M_\infty^2|^{1.7574}\right)^{\frac{2}{3}}+|1-M_\infty^2|^{1.1716}\right] \qquad (63)$$

the equation above will allow us to plot $K(\tilde{x})$ vs. $\tilde{x}$ in Fig.(5) for M_∞ = 1.05, 1.1, and 1.2. Where $K(\tilde{x}) < 0$ for $M_\infty \geq 1.0$ and $K(\tilde{x}) > 0$ for $M_\infty < 1.0$.

Therefore, integrating both sides of equation (58) becomes

$$\int_{\tilde{r}_0}^{\tilde{r}} \frac{d\tilde{r}}{\left[\frac{8}{\tilde{r}^3} - 2.8284\left|1-M_\infty^2\right|\tilde{r}^{1.8284} - .1512\,(1-M_\infty^2)^2\tilde{r}^{6.657}\right]} = \frac{-3.26x10^{-2}}{M_\infty^2(\gamma+1)}\int_0^{\tilde{x}} \xi\, d\tilde{x} \tag{64}$$

Equation(64) is numerically integrated and which then allows us to determine the boundary surfaces in dimensionalize and non-dimensionalize (normalize) form as shown in Figs. 6 and 7 for M_∞ = 1.05, 1.1, and 1.2. Now, we can determine C_p from Eqn.(40) and local Mach number from Eqn.(49) for the three surfaces obtained at different Mach numbers.

In Figs. 8-13, the supersonic boundary surfaces for M_∞=1.05,1.10, and 1.20 are plotted with their pressure coefficients and local Mach profiles in dimensionalized and non-dimensionalized (normalized) form. These results will be verified later using a 3-D Navier-Stokes solver in Computational Fluid Dynamics (CFD).

V. SONIC BOUNDARY SURFACE

The sonic flow (M_∞=1.0) can be derived in explicit form from Equations (24) and (25). The resulting equations for sonic flow are

$$\bar{x} = \int \frac{d\xi}{\xi^{\frac{2}{3}}} \tag{65}$$

and

$$\zeta = \frac{4}{\bar{r}^2} \tag{66}$$

Rearranging Equation (65)

$$\bar{x} = \int_0^{\xi} z^{-\frac{2}{3}}\, dz \tag{67}$$

since Equation (67) is integrable, we obtain

$$\bar{x} = 3\, \xi^{\frac{1}{3}} \tag{68}$$

or

$$\xi = \frac{\bar{x}^3}{27} \tag{69}$$

We can write Equations (11) and (13) in sonic form as

$$x = \int \frac{d\xi}{\left(\frac{3}{2}\,\lambda\,\xi^2\right)^{\frac{1}{3}}} \tag{70}$$

and

$$\zeta = \frac{4}{\lambda\, r^2} \tag{71}$$

integrating Equation (70), we have

$$\xi(x) = \frac{1}{18}\,\lambda\, x^3 \tag{72}$$

From Equation (4), we can write the sonic perturbation potential as

$$\varphi(x,r) = \xi(x)\,\zeta(r) \tag{73}$$

Substituting Equations (71) and (72) into Equation (73) yields

$$\varphi(x,r) = \frac{2}{9}\frac{x^3}{r^2} \tag{74}$$

Equation (57) can be written for M_∞=1.0 as

$$\frac{d\bar{r}}{d\bar{x}} = \frac{-\,0.2608}{(\gamma+1)}\frac{\bar{\xi}}{\bar{r}^3} \tag{75}$$

Rearranging Equation (75), we have

$$\tilde{r}^3 \, d\tilde{r} = -0.1087 \, \xi \, d\tilde{x} \tag{76}$$

Therefore, integrating both sides of Equation (76), we obtain

$$\int_{\tilde{r}_0}^{\tilde{r}} \tilde{r}^3 \, d\tilde{r} = -0.1087 \int_0^{\tilde{x}} \xi \, d\tilde{x} \tag{77}$$

Inserting Equation (69) into Equation (77) yields

$$\tilde{r}^4 - \tilde{r}_0^4 = -0.0040 \, \tilde{x}^4 \tag{78}$$

where $\tilde{r}_0 = 4.0$ has been chosen as an asymptotic value to represent the condition sufficiently well at $M_\infty = 1.0$. Equation (78) will allow us to determine sonic boundary surface.
The pressure coefficient can be written from Eqn.(40) as

$$C_p = \frac{-0.4416}{(\gamma+1)} \zeta \, \xi^{\frac{2}{3}} \tag{79}$$

in case of $M_\infty = 1.0$.

The local Mach number can be written from Equation (49) for the sonic surface as

$$M^2 = \frac{(1 - C_p)}{\left(1 + \frac{\gamma - 1}{2} C_p\right)} \tag{80}$$

The sonic surface is represented dimensionally in Fig. (14) with the pressure coefficient and local Mach number profiles, and normalized in Fig. (15) with $\bar{r}_o = 4.0$ for ($M_\infty = 1.0$). The sonic boundary surfaces, in both forms, are plotted with the supersonic boundary surfaces in Figs. 16 and 17.

VI. COMPUTATIONAL FLUID DYNAMICS (CFD)

The history of Computational Fluid Dynamics (CFD) is closely tied to the rapid advances in digital computer which has a great impact on problems of design in modern engineering practice. These problems can now be solved at very little cost in a few seconds of computer time which would have taken years to work out with the computational methods and computers available twenty years ago. [Ref. 8]

The CFD will be used to compute the axi-symmetric flow over the boundary surfaces obtained by the small perturbation method.

The computer program GRAPE [Ref.9], an acronym derived from Grids about Airfoils using Poisson's Equation, has been written by R. Sorenson at Ames Research Center to generate two-dimensional finite difference grids about airfoils and other shapes by the use of the Poisson differential equation. Outer and inner boundaries are specified for the C-type grid, where the surface of the body is treated as the inner boundary. Important characteristics in grid generation are the ability to specify the spacing between mesh points at the boundary, in the direction normal to the boundary, and the control of the angles with which mesh lines intersect the boundaries which is known as orthogonality.

The grid size for the sonic surface (M_∞=1.0) is 107 x 60 and for the supersonic surfaces (M_∞=1.1, 1.2) is 115 x 60 as shown in Fig.(18). Since the surfaces are symmetrical, half of the grid or eventually the lower surface was rotated for 11 planes plus two more for symmetry to generate an axi-symmetric after body surface.

The OVERFLOW program [Ref.10] developed by Ames Research Center which uses 3-D Navier-Stokes and Euler solver for viscous/ inviscid flow was applied. The results are shown in Figs. 19-21 for three different boundary surfaces at M_∞ = 1.0, 1.1, and 1.2 with 1500 iterations. It was found that the density residuals decreased by more than one order of magnitude over 1500 iterations. After 3000 iterations, the solution converged by two orders of magnitude.

In case of the sonic surface Fig.(19) with M_∞=1.0, the Mach lines contour shows the shock is forming downstream at a local Mach M=1.65 at which the flow becomes subsonic downstream of the shock. This result complies with the small perturbation transonic solution obtained earlier in Fig.(15). In other words, the flow is shock free over the sonic surface in for M_∞=1.0.

For the supersonic boundary surfaces M_∞=1.10, and 1.20, we can see that the flow starts at M=1.10 and M=1.20 respectively and follows the afterbody surface until it shocks. The shock is formed at local Mach M=1.75 and 1.85 respectively as shown in Figs. 20 and 21.

On the other hand, these results agree with the small perturbation solution over the transonic range as plotted in Figs. 11 and 13 where the local Mach is represented by the dash line and it is increasing towards the afterbody surface until it shocks. This indicates that the flow is shockless over these supersonic boundary surfaces in the transonic regime.

The velocity vectors are plotted in Fig.(22) for M_∞=1.0 which shows that the flow is following the afterbody surface until the shock, and then flow separation takes place due to the steep pressure rise and the introduction of numerical viscosity into the flowfield at this location.

These boundary surfaces obtained are of interest for design of body of revolution such as missiles afterbody or aircraft engines, in which a patching technique may be applied to these surfaces to get the best shockless surface in the transonic range.

VII. CONCLUSION AND RECOMMENDATION

We have shown in this research a solution to the non-linear transonic small perturbation equation by implementing the separation of variables technique. The x-dependence was integrated numerically and the r-dependence was solved by an outer expansion method. It was found that the parameter $(1-M_\infty^2)$ has strong effect in specifying the shape of the boundary surfaces of interest for design. A 3-D viscous/ inviscid Navier-Stokes/ Euler solver in Computational Fluid Dynamics (CFD) confirmed our results obtained from the small perturbation technique for the boundary surfaces at M_∞=1.0, 1.10, and 1.20 . *In other words, we achieved our goal of designing shockless surface in the transonic range.*

This research may be extended using a patching technique to obtain the best shockless surface in the transonic flows. Patching criteria will have to be developed based on the mathematics and the flow constraints. Also, connection between small perturbation solution and CFD might eventually be done internally in the computer. The small perturbation is the most efficient method to define or to design axi-symmetric afterbody transonic surfaces, however CFD can be used to predict the performance of these aerodynamic surfaces.

LIST OF REFERENCES

1. Biblarz, O., "Phase Plane Analysis of Transonic Flows," AIAA, paper no. 76-332, July 1976; also unpublished paper, Naval Postgraduate School, 1992.

2. Van Dyke, M.D., "Perturbation Methods in Fluid Mechanics," Academic Press, N.Y. 1964.

3. Guderley, K. G., "The Theory of Transonic Flow," Pergamon Press, London 1962.

4. Liepmann, H.W., Roshko, A., "Elements of Gas Dynamics," John Wiley and Sons, Inc. 1957.

5. Zucrow, M. J., Hoffman, J.D., "Gas Dynamics." Vol. I & II, John Wiley and Sons, Inc. 1976.

6. Salama, A., "Two-Dimensional Boundary Surfaces For Planar External Transonic Flows," Naval Postgraduate School, 1992.

7. Nixon, D., "Transonic Aerodynamics," AIAA, Progress in Astronautics and Aeronautics, vol. 81, 1982.

8. Anderson, A.D., Tannehill, C.J., and Pletcher, H.R. "Computational Fluid Mechanics and Heat Transfer," Hemisphere Publishing Corporation, 1984.

9. Sorenson, R.L., "A Computer Program to Generate Two-Dimensional Grids About Airfoils and Other Shapes by the use of Poisson's Equation," NASA Technical Memorandum 81198, 1981.

10. Bunning, P.G., and others, "Overflow User's Manual Version 1.6t," NASA AMES Research Center, California, 29 June, 1992.

APPENDIX A

FIGURES

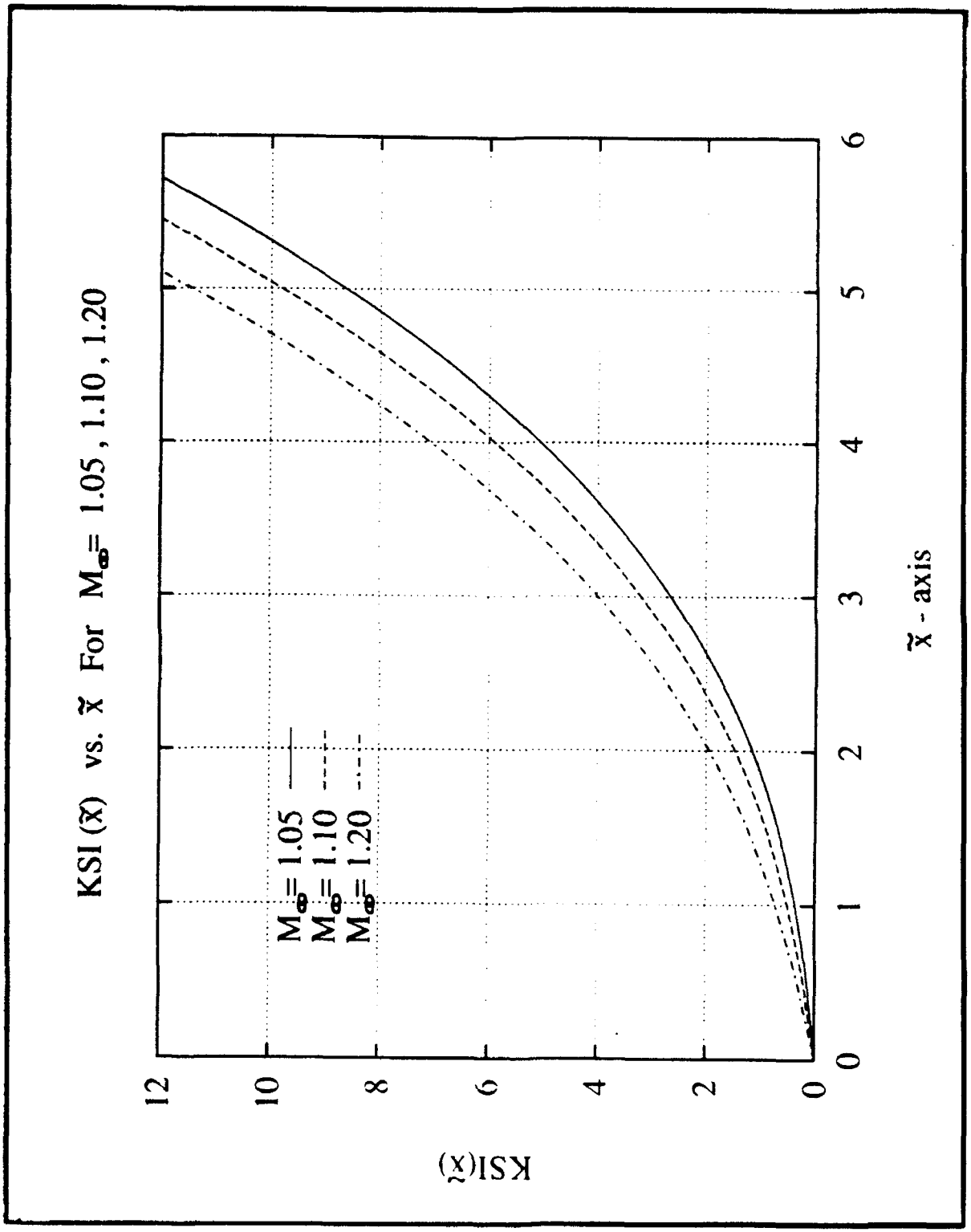

Figure 1. Numerical integration of Eqn. 24.

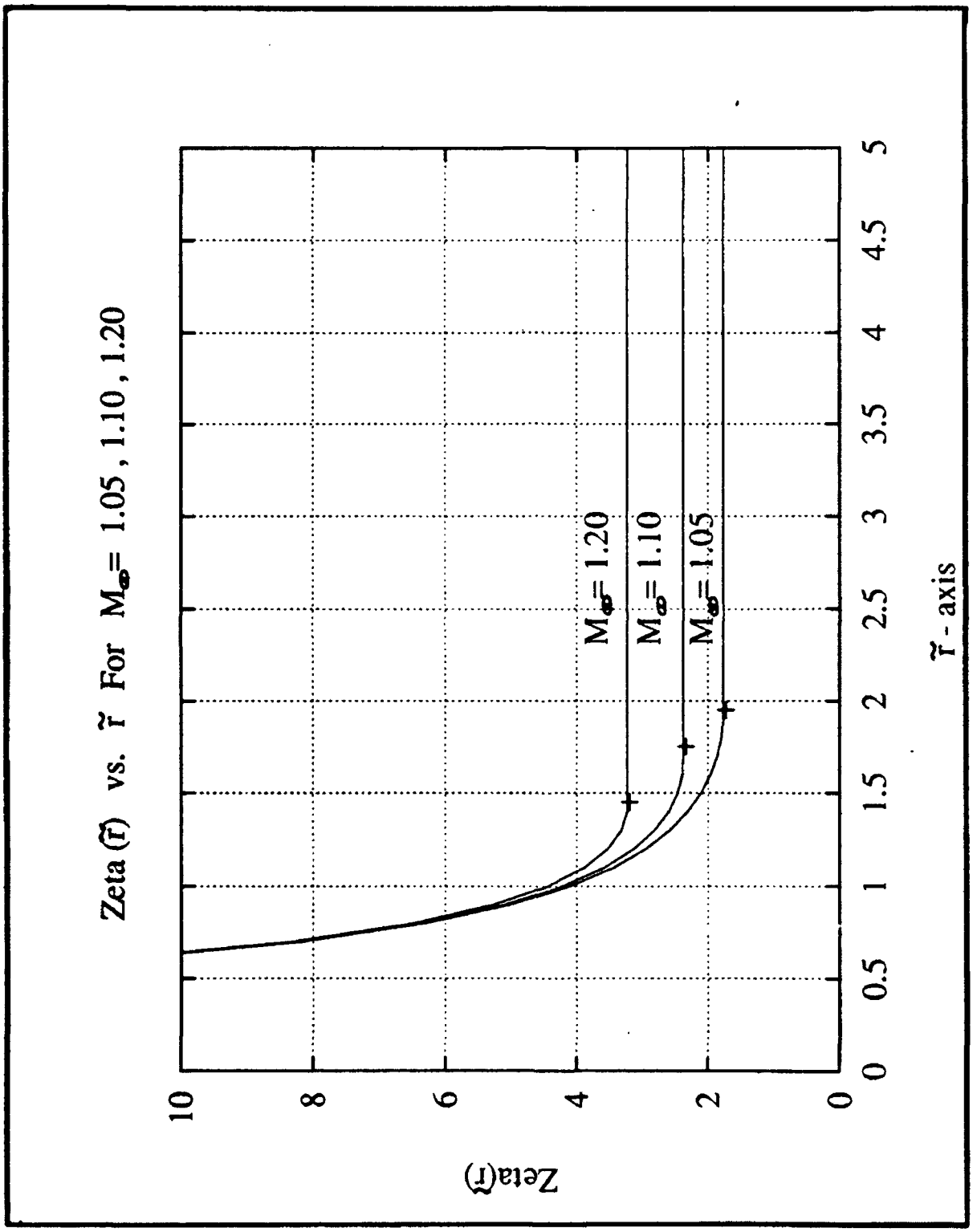

Figure 2. Numerical solution of Eqn. 25.

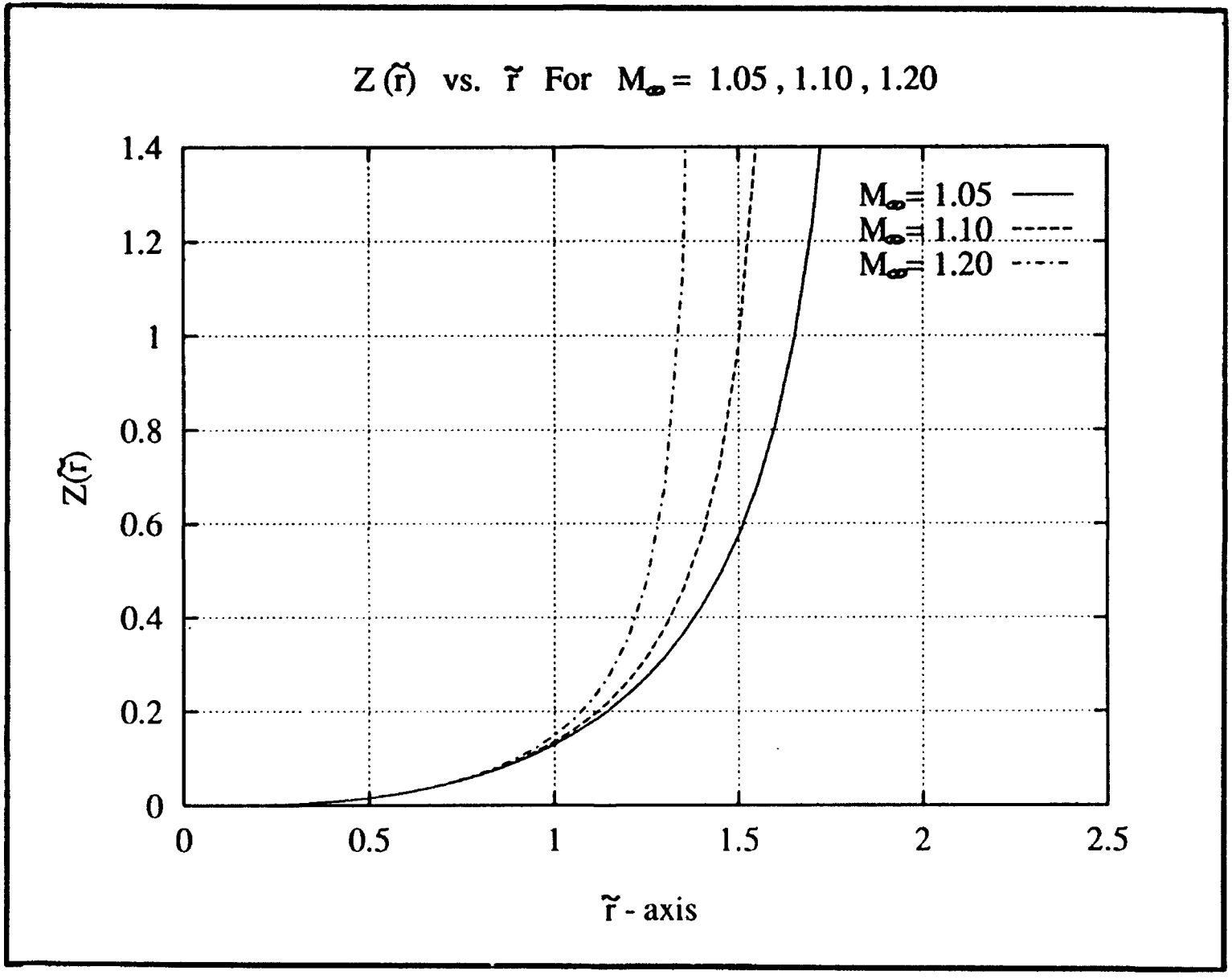

Figure 3. Numerical solution of Eqn. 59.

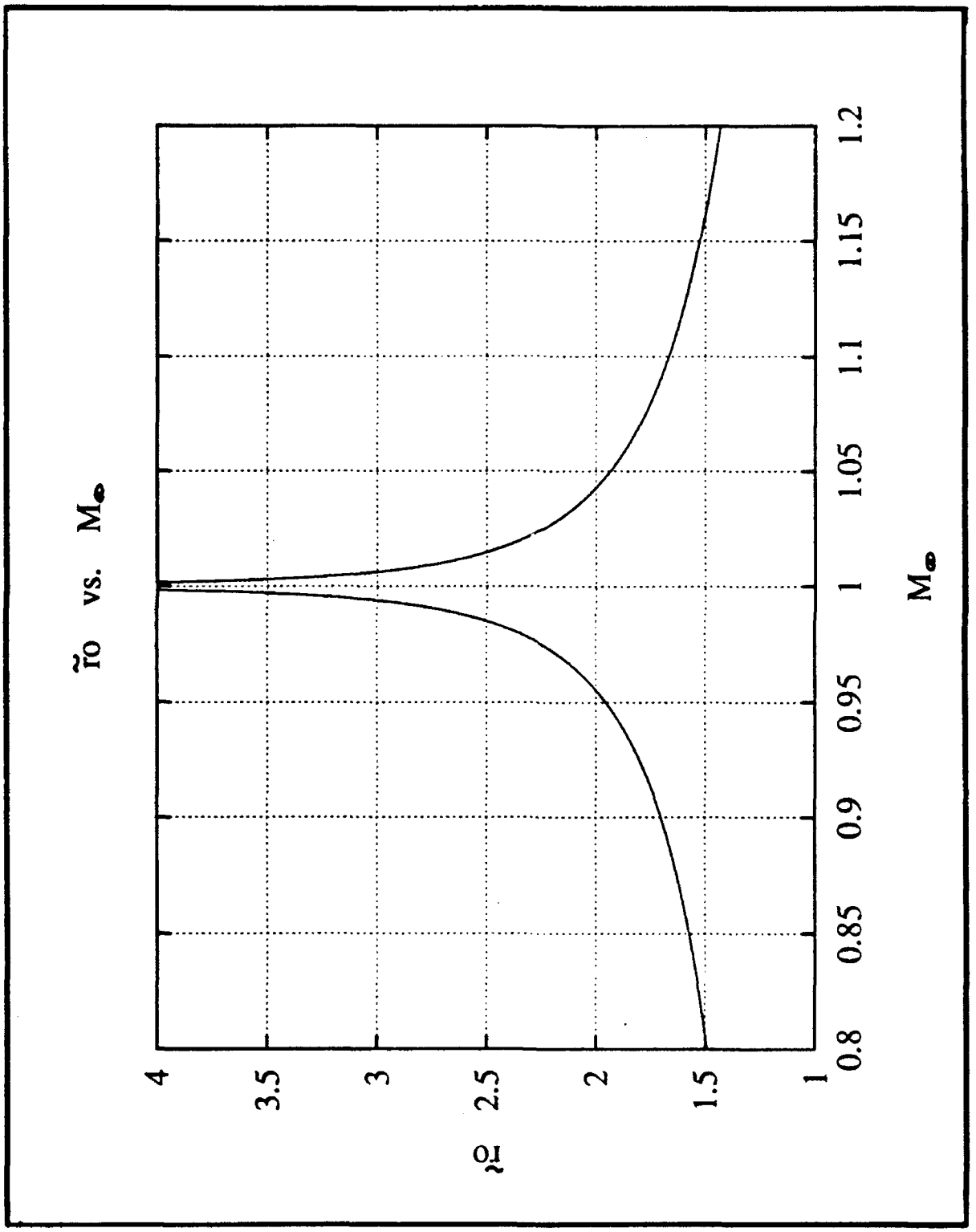

Figure 4. Numerical solution of Eqn. 60.

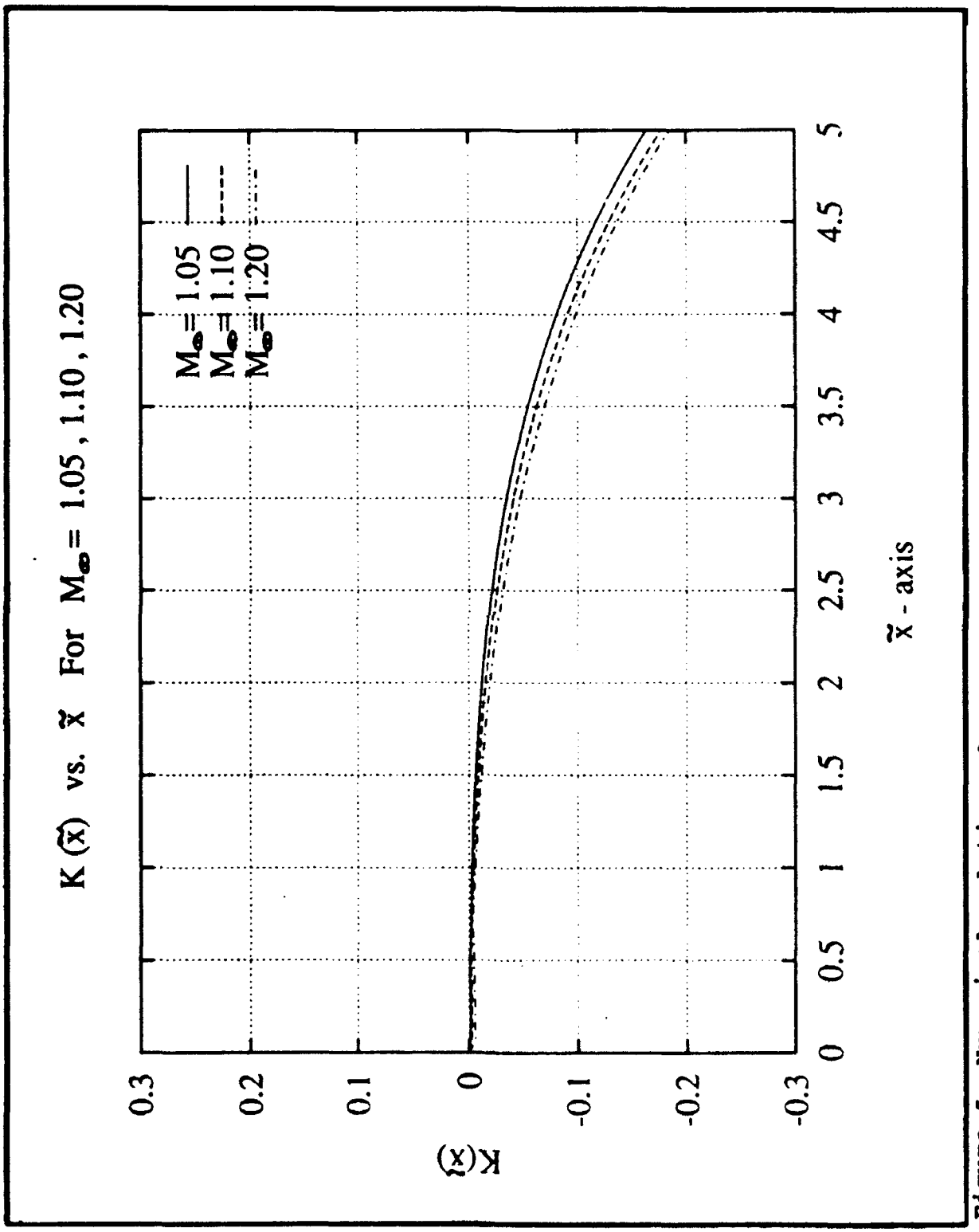

Figure 5. Numerical solution of Eqn. 63.

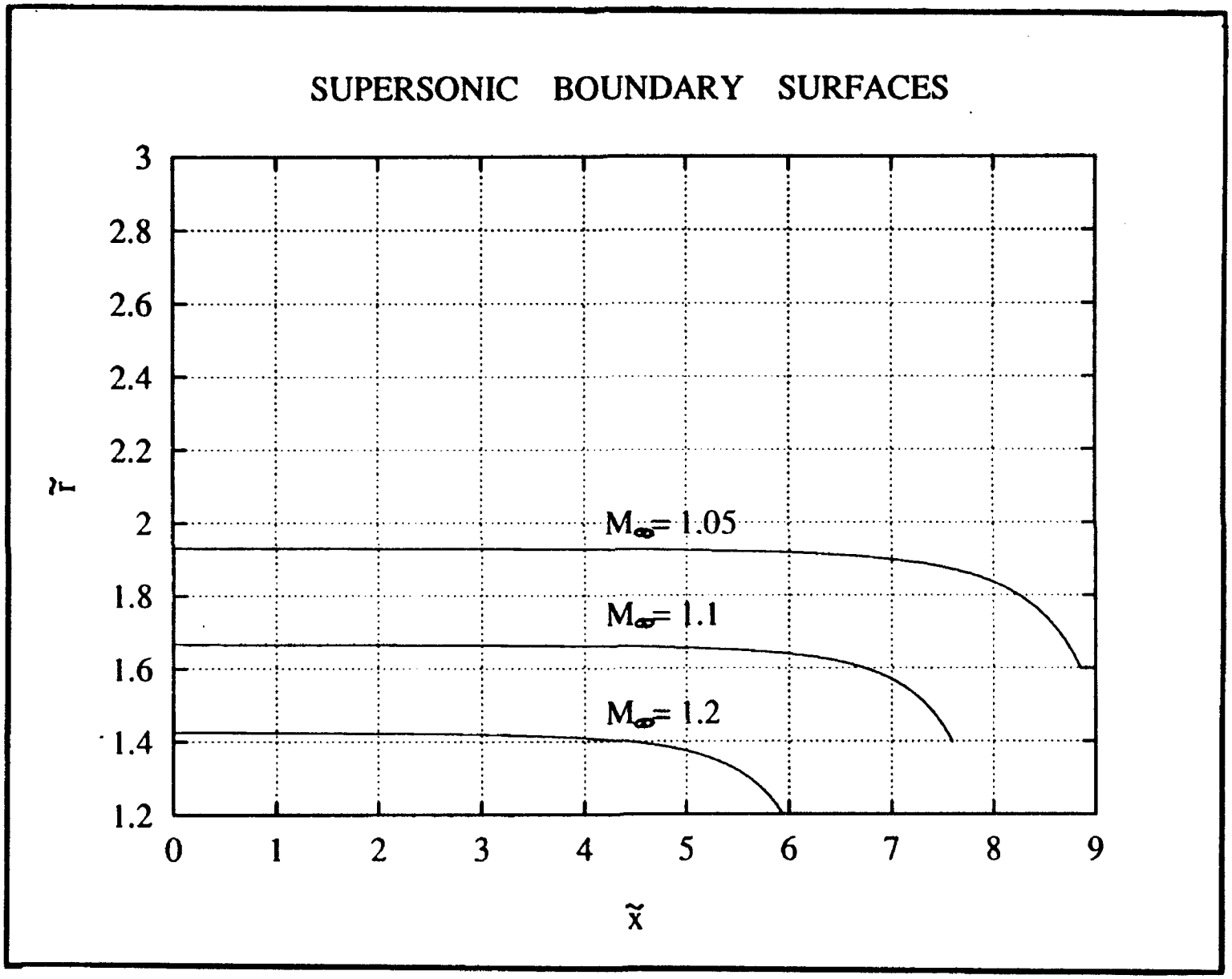

Figure 6. Numerical solution of Eqn. 64.

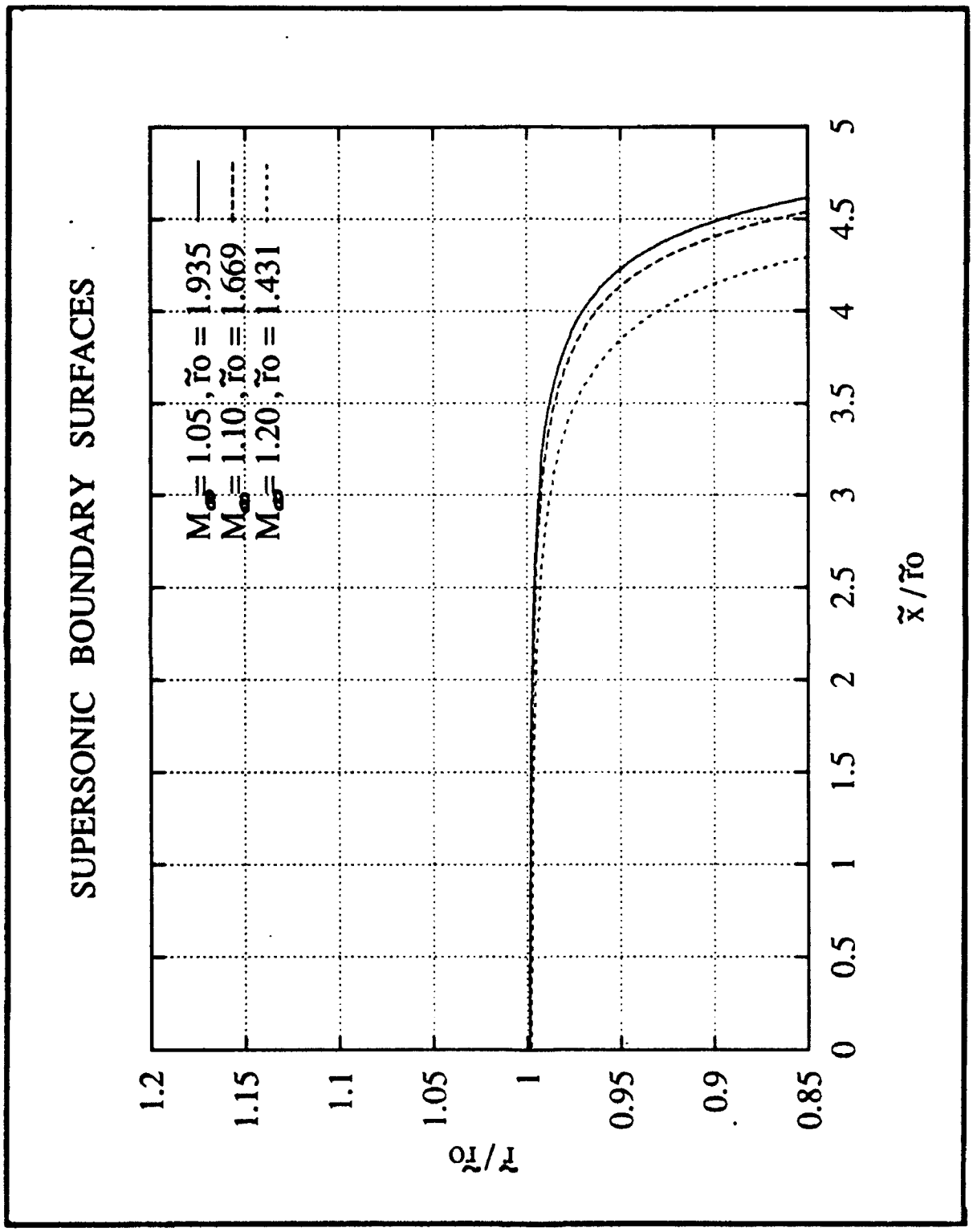

Figure 7. Numerical solution of Eqn. 64 (normalized).

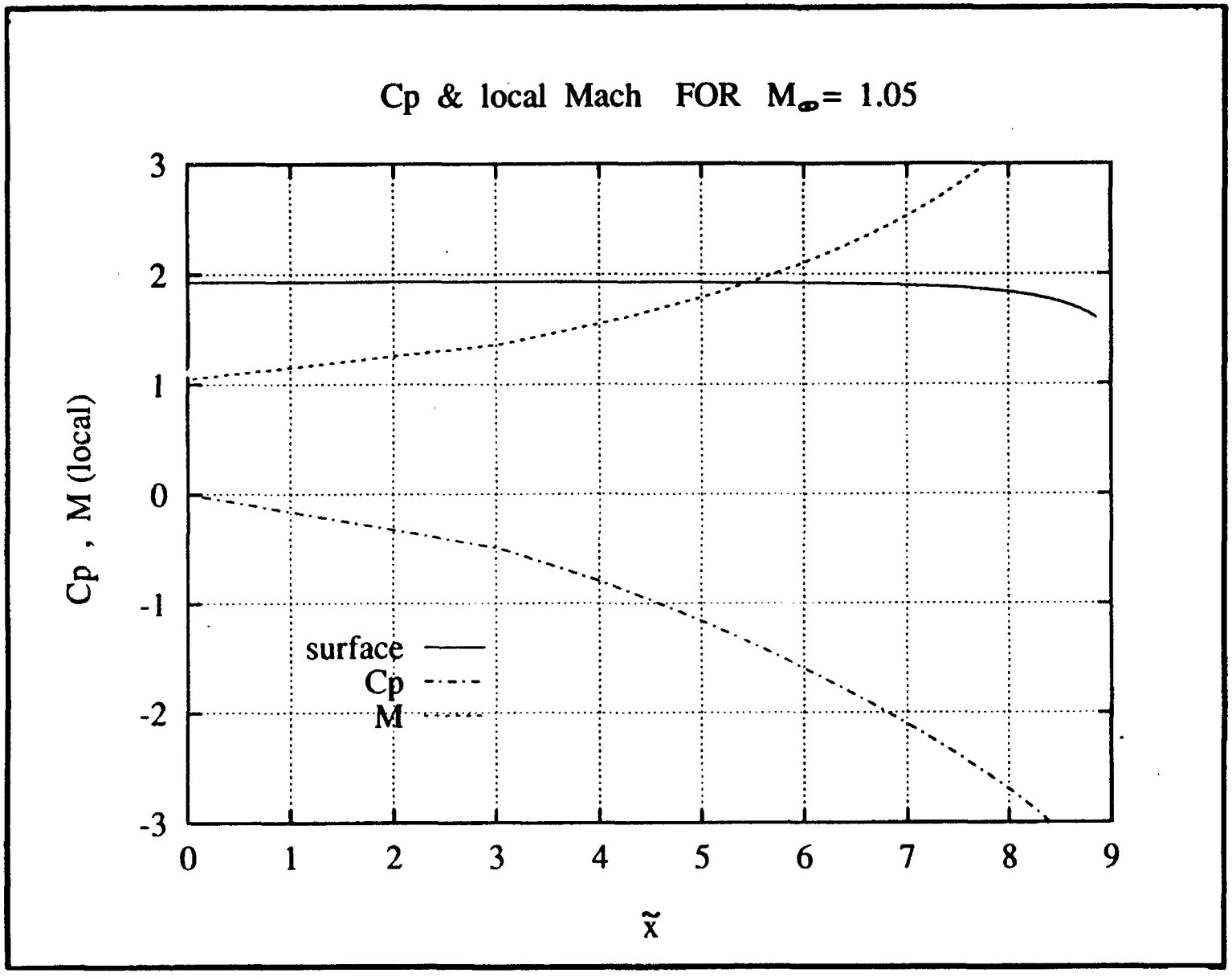

Figure 8. Cp and local Mach for M_∞ = 1.05.

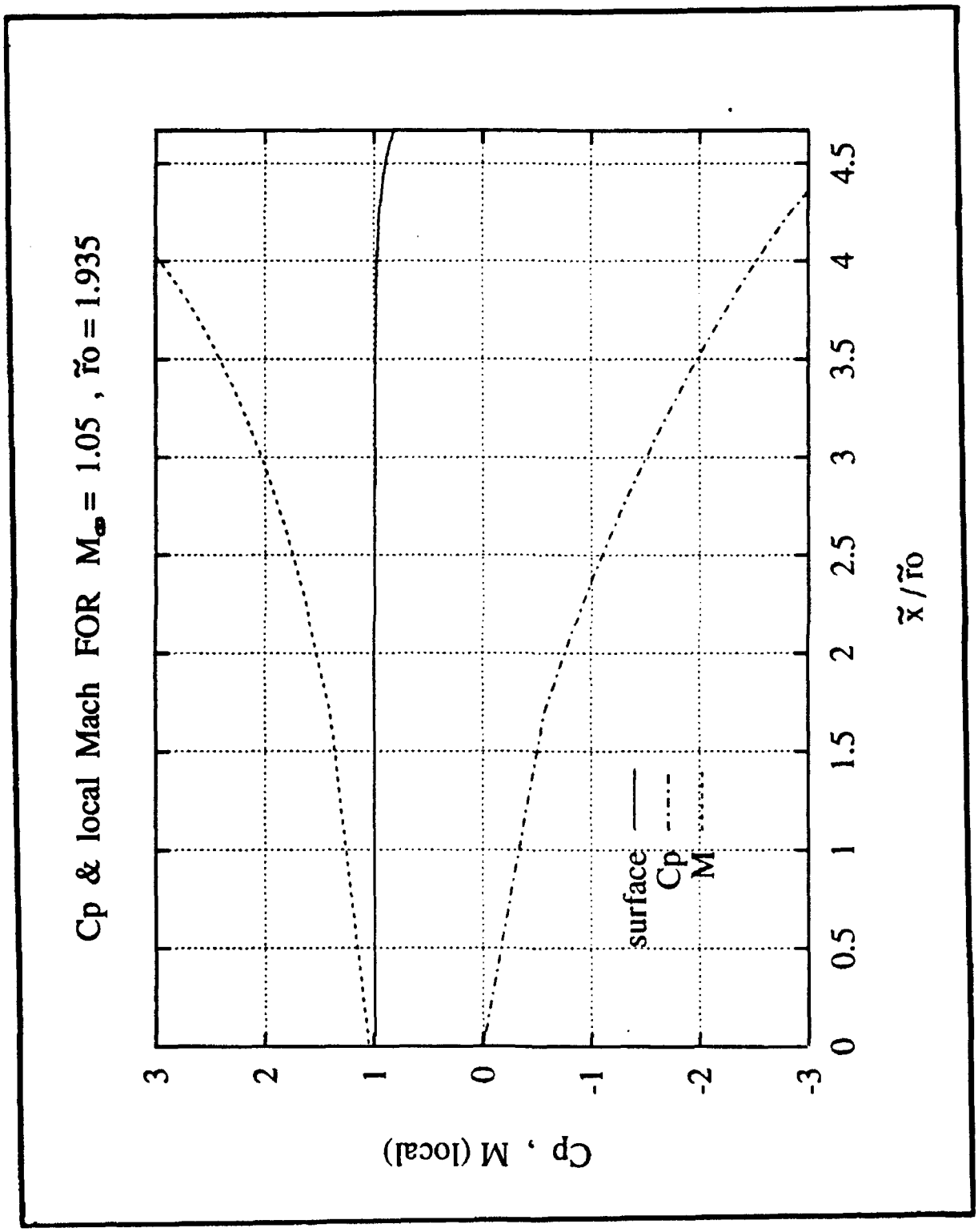

Figure 9. Cp and local Mach for M_∞ = 1.05 (normalized).

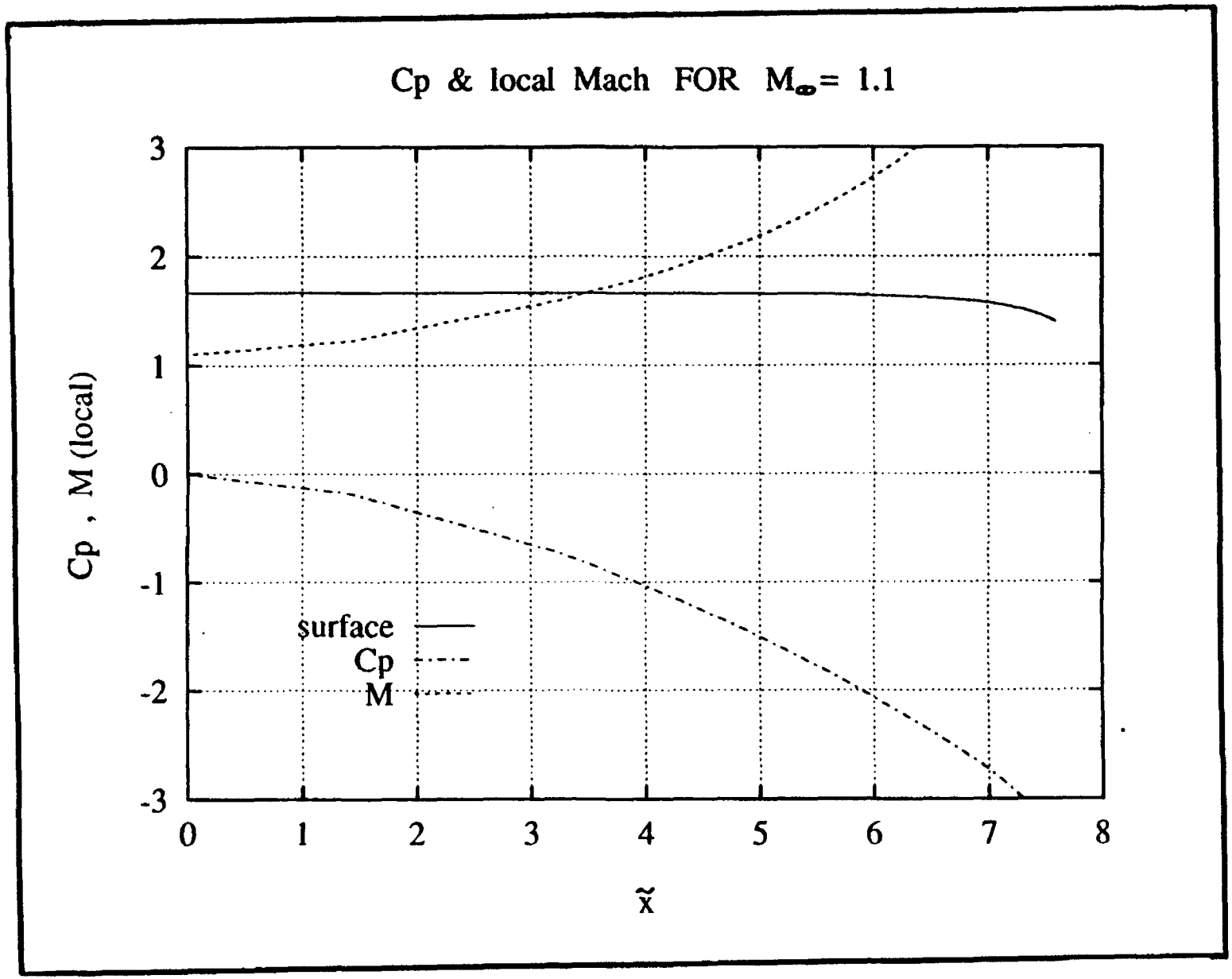

Figure 10. Cp and local Mach for M_∞ = 1.10.

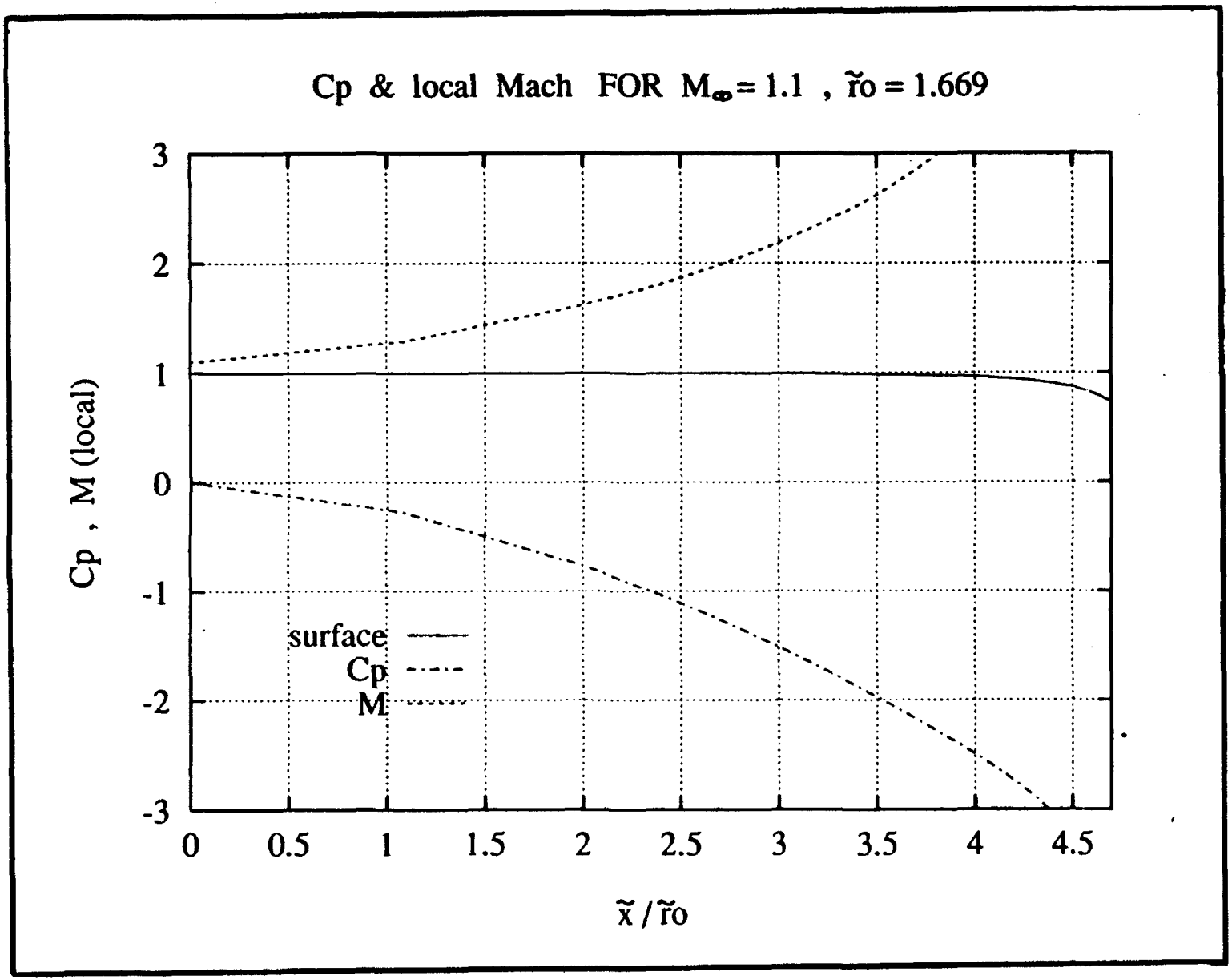

Figure 11. Cp and local Mach for M_∞ = 1.10 (normalized).

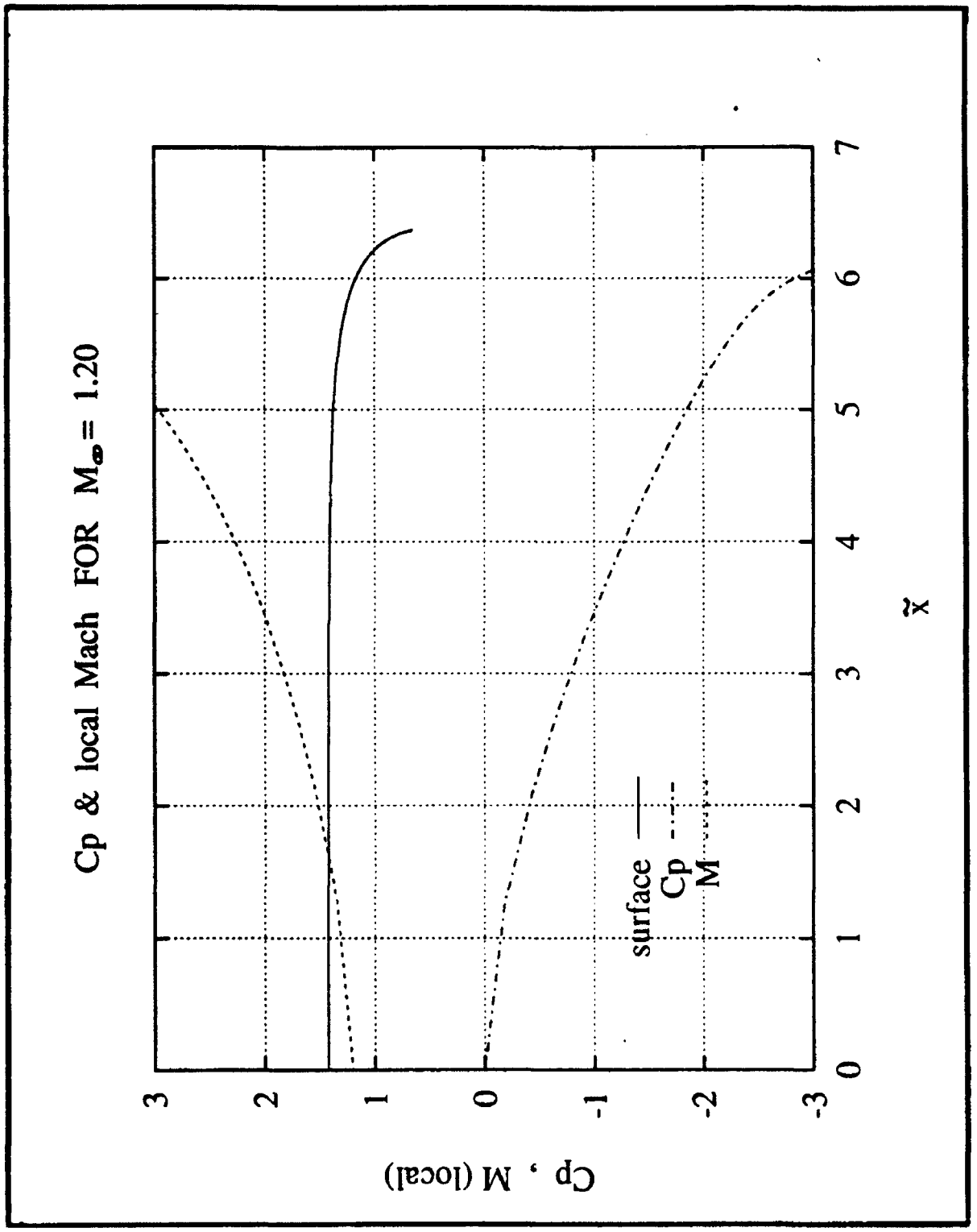

Figure 12. Cp and local Mach for M_∞ = 1.20.

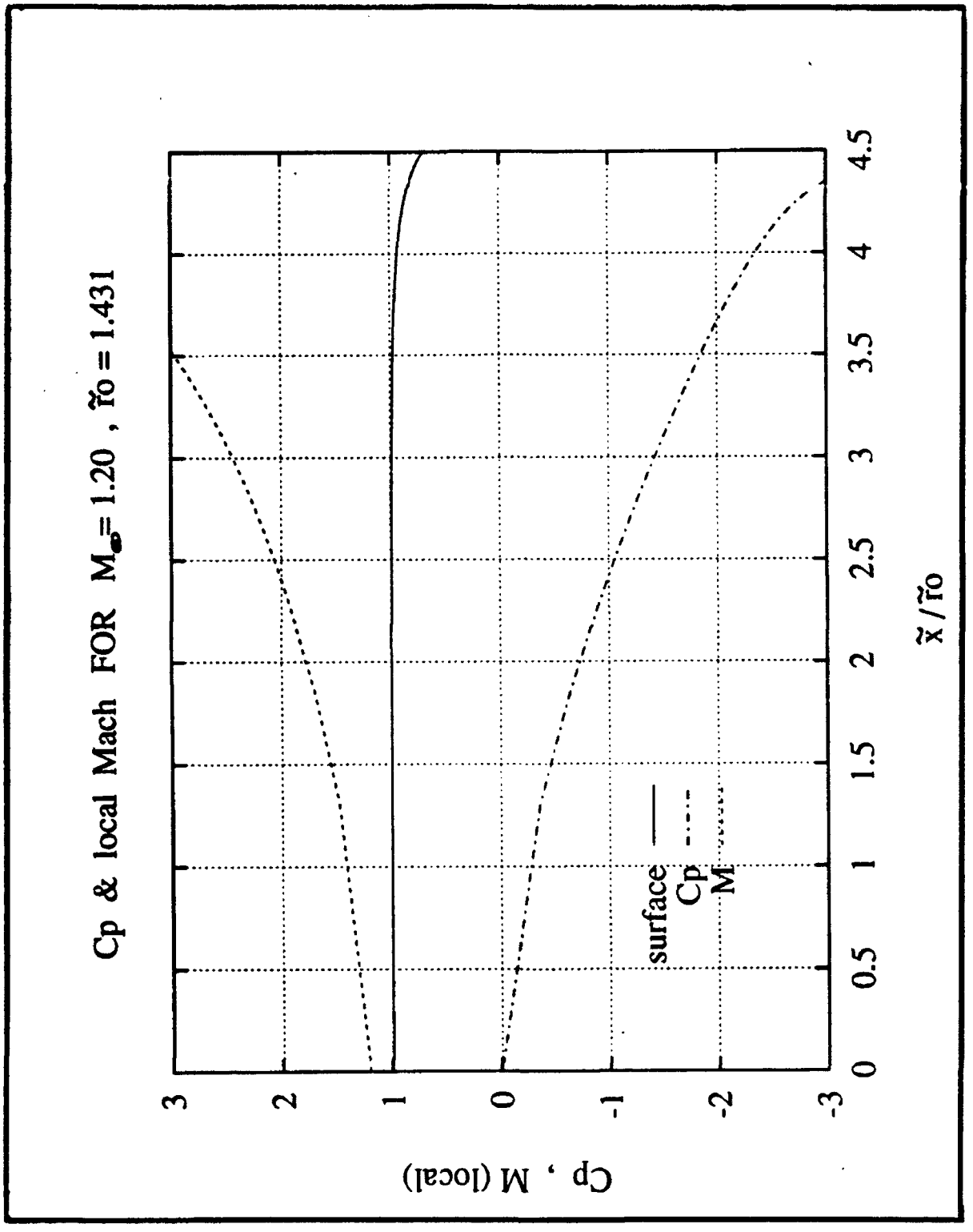

Figure 13. Cp and local Mach for M_∞ = 1.20 (normalized).

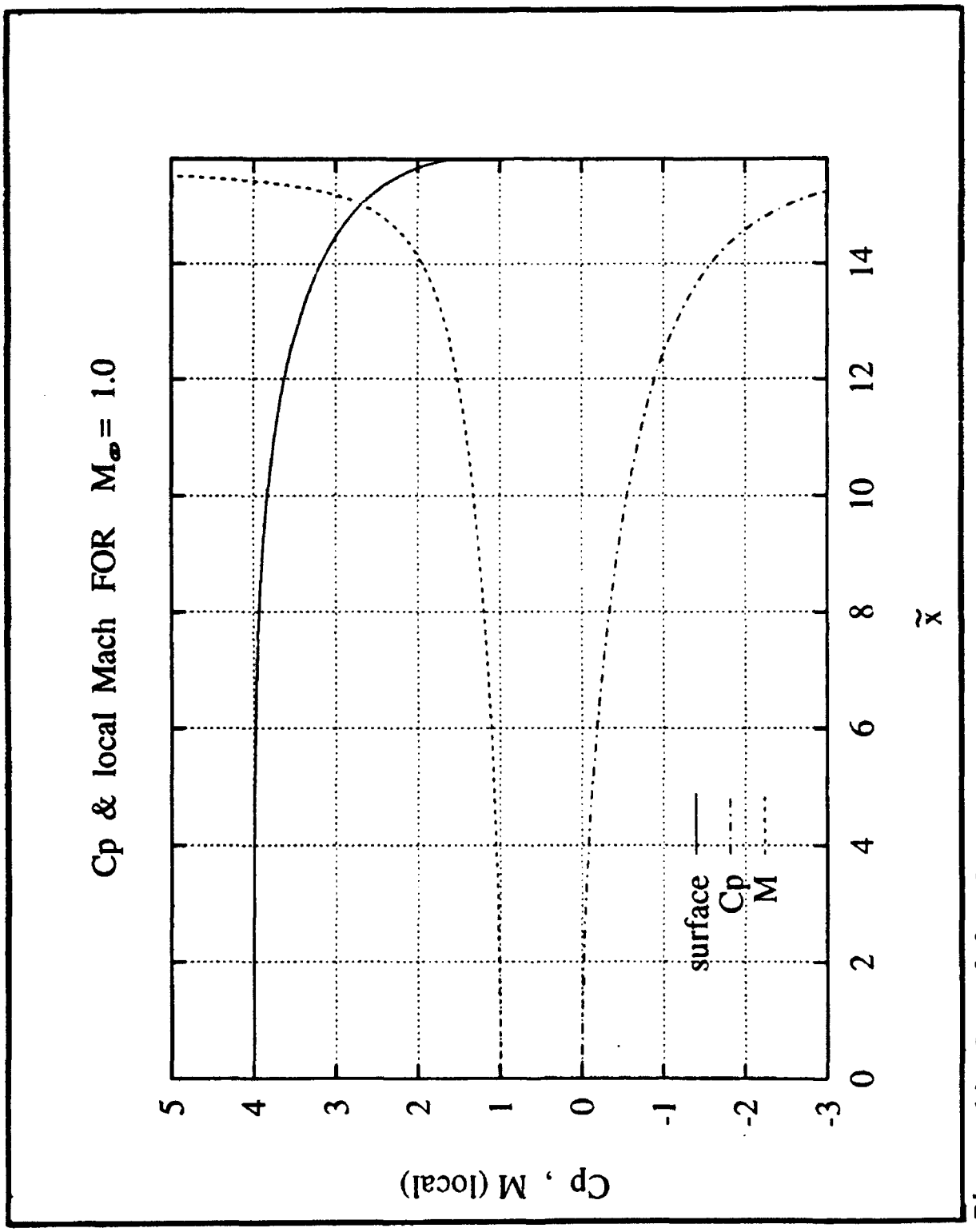

Figure 14. Cp and local Mach for M_∞ = 1.0.

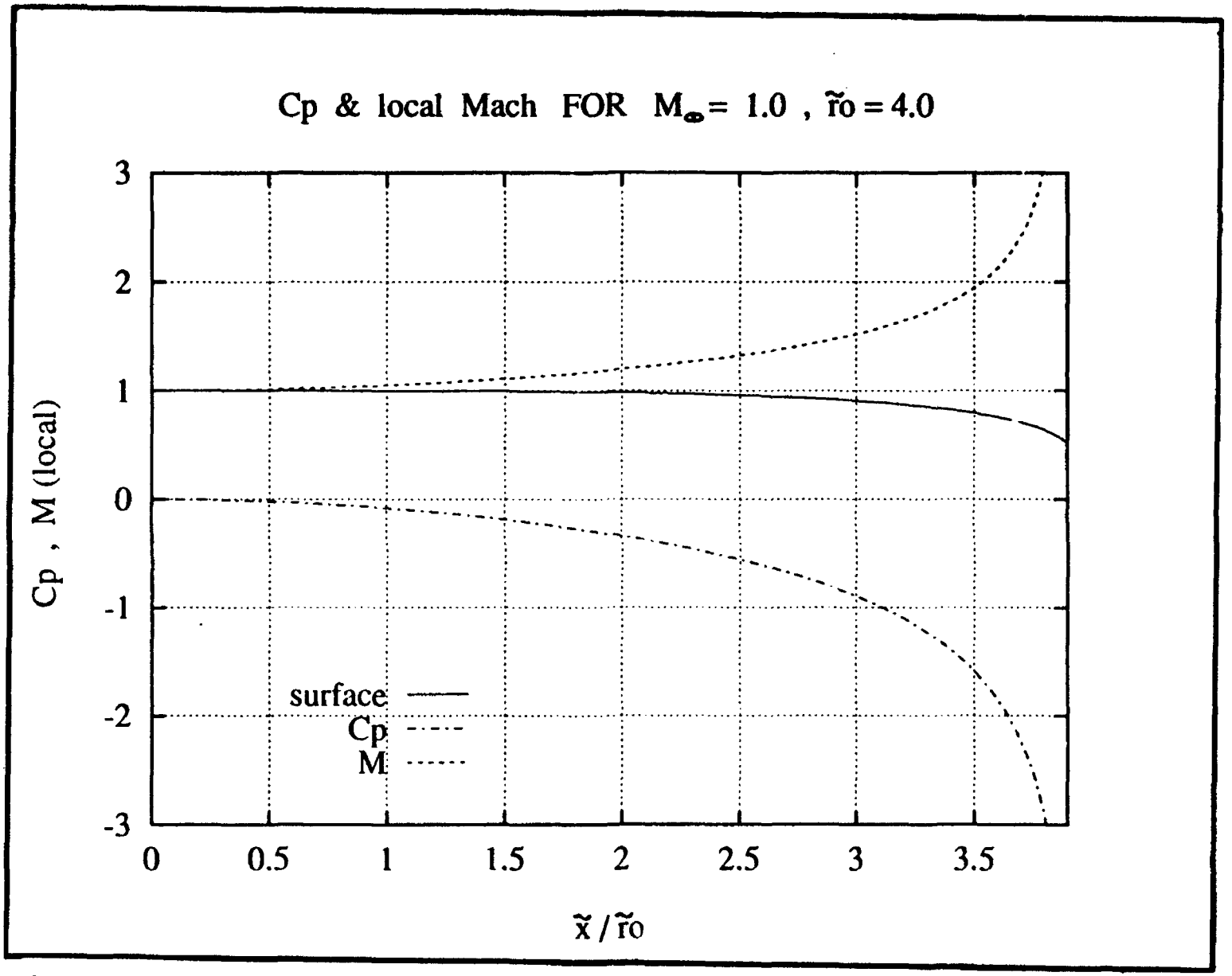

Figure 15. Cp and local Mach for M_∞ = 1.0 (normalized).

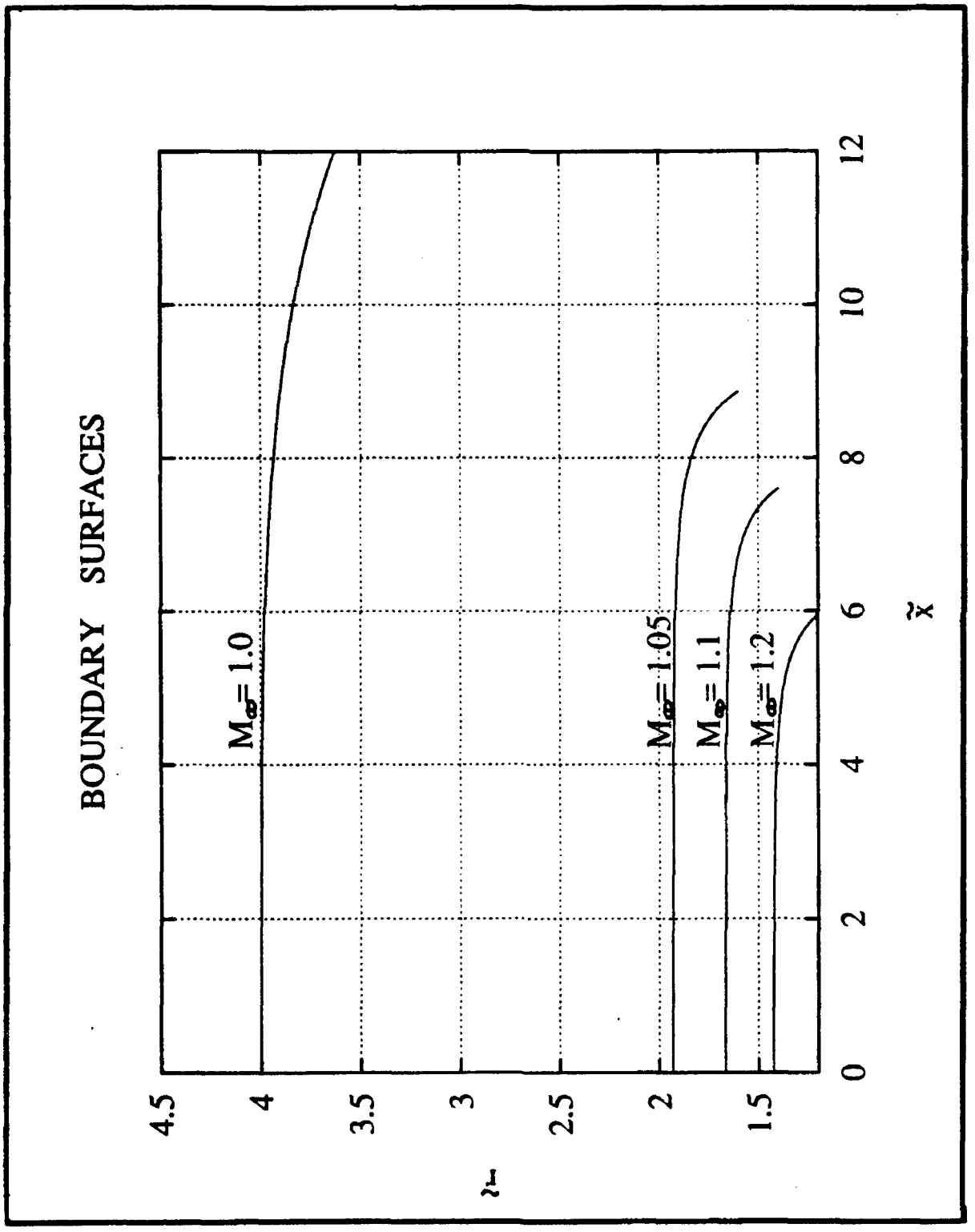

Figure 16. Boundary surfaces for M_∞ = 1.0,1.05,1.1,1.2.

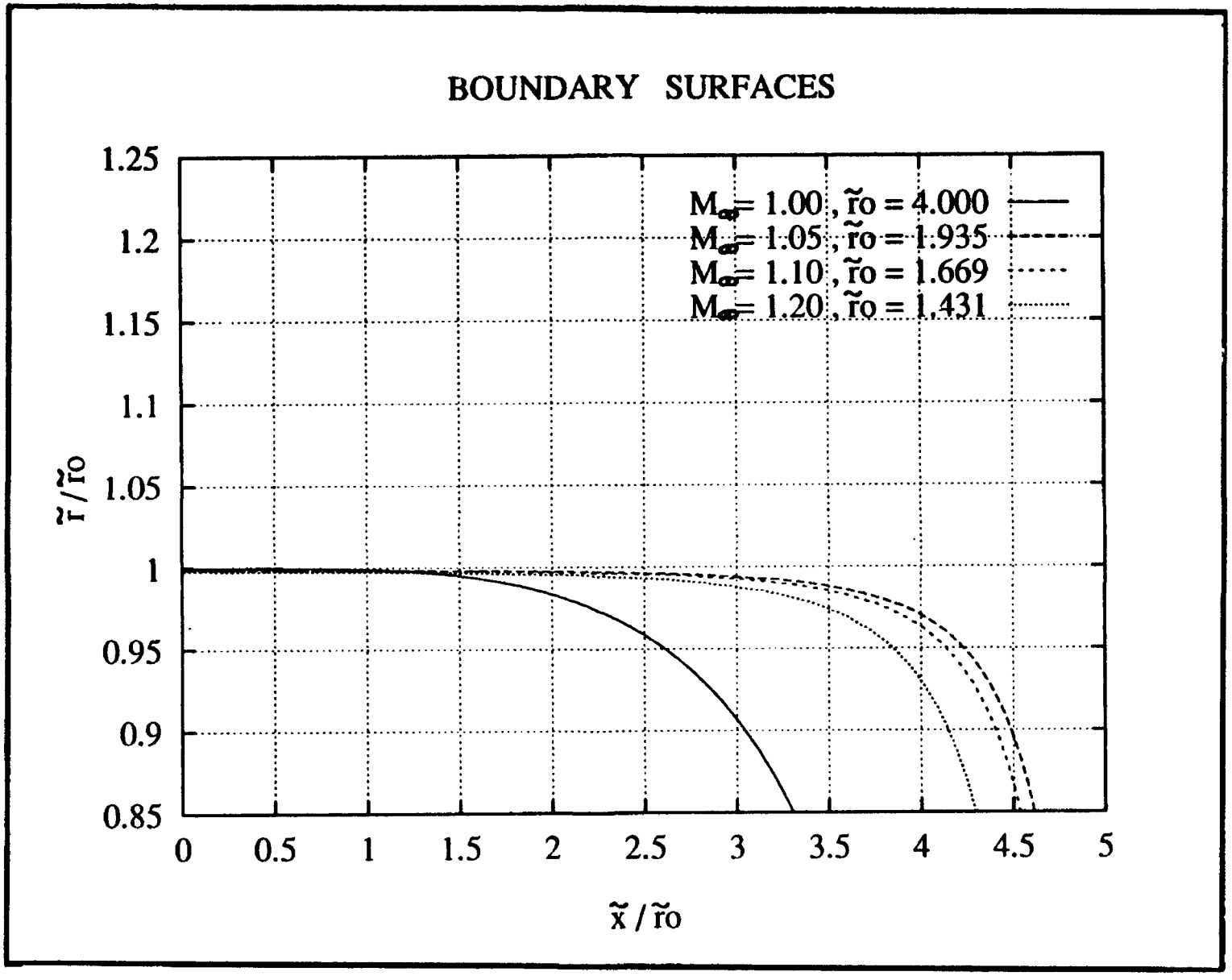

Figure 17. Boundary surfaces for M_∞ = 1.0,1.05,1.1,1.2(normalized).

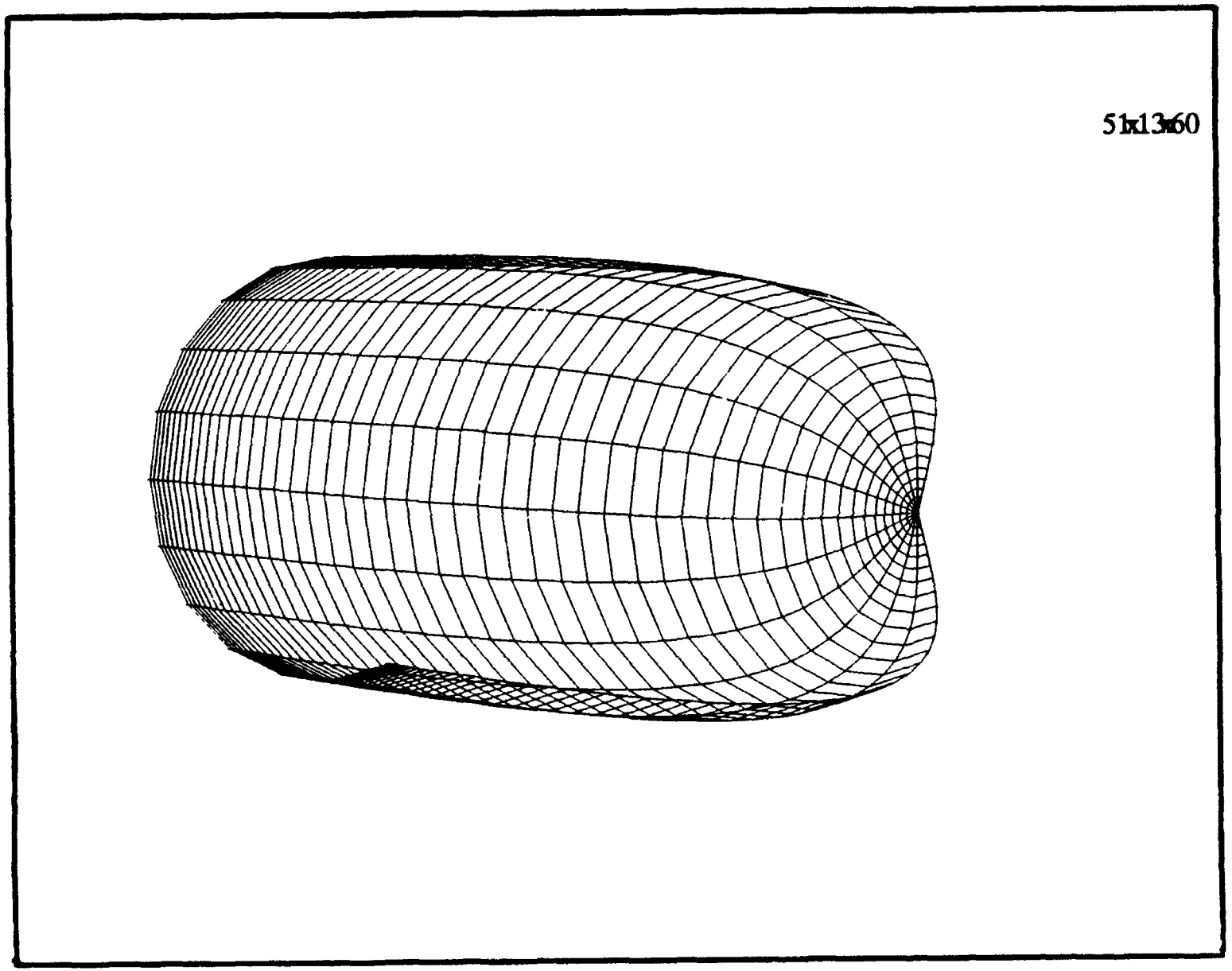

Figure 18. Afterbody axi-symmetric grid.

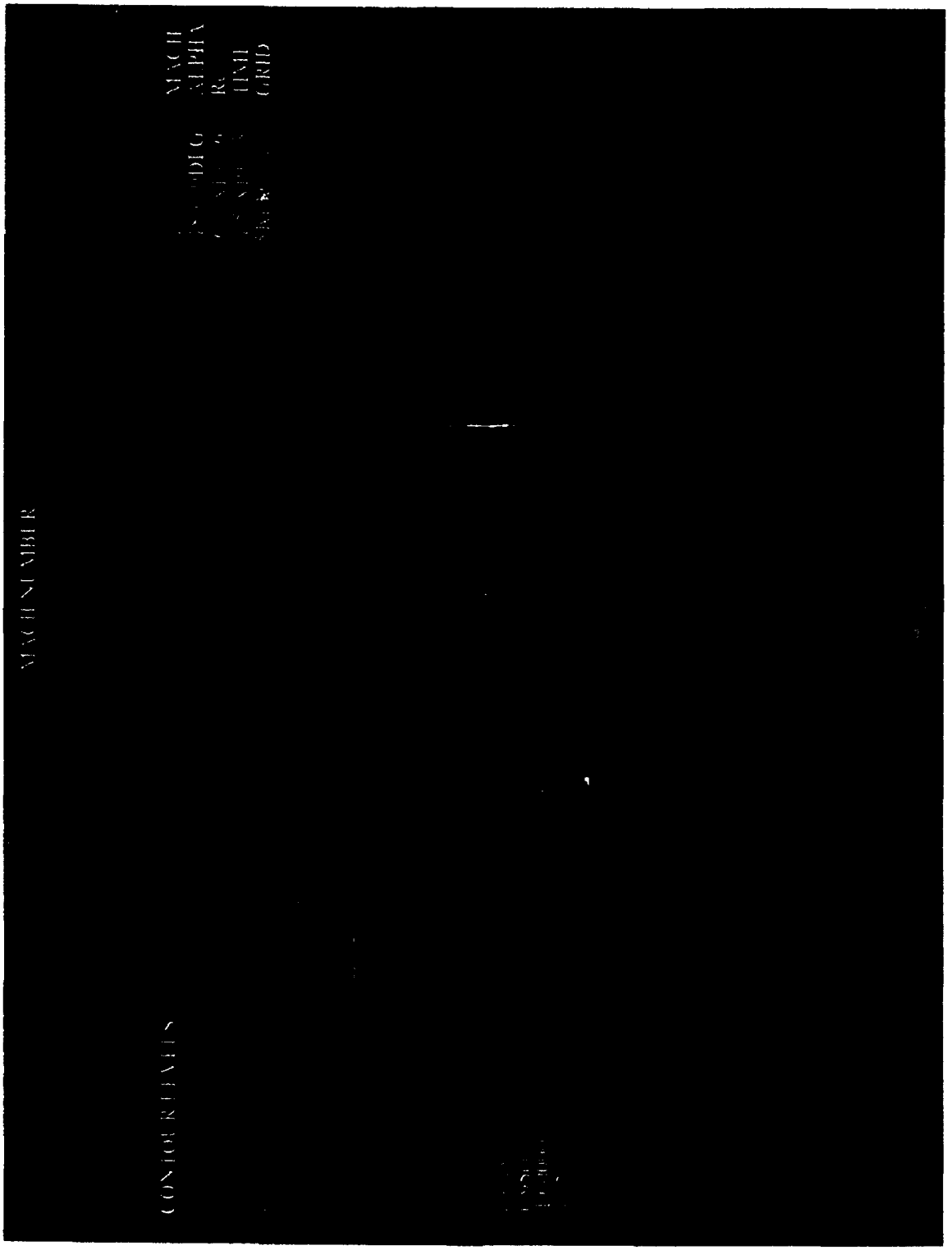

FIGURE 19. MACH CONTOURS FOR M =1.0.

FIGURE 20. MACH CONTOURS FOR M =1.10.

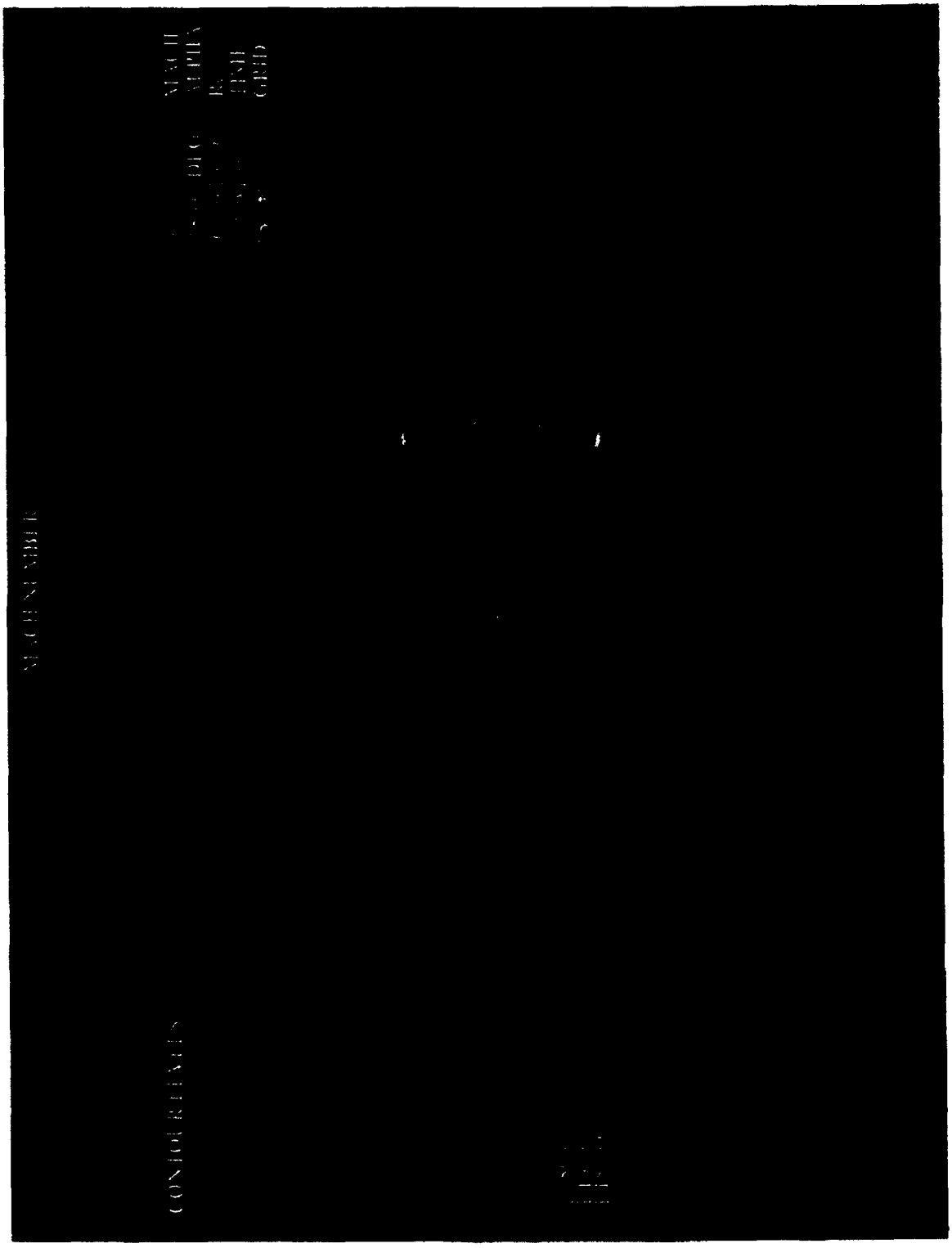

FIGURE 21. MACH CONTOURS FOR M =1.20.

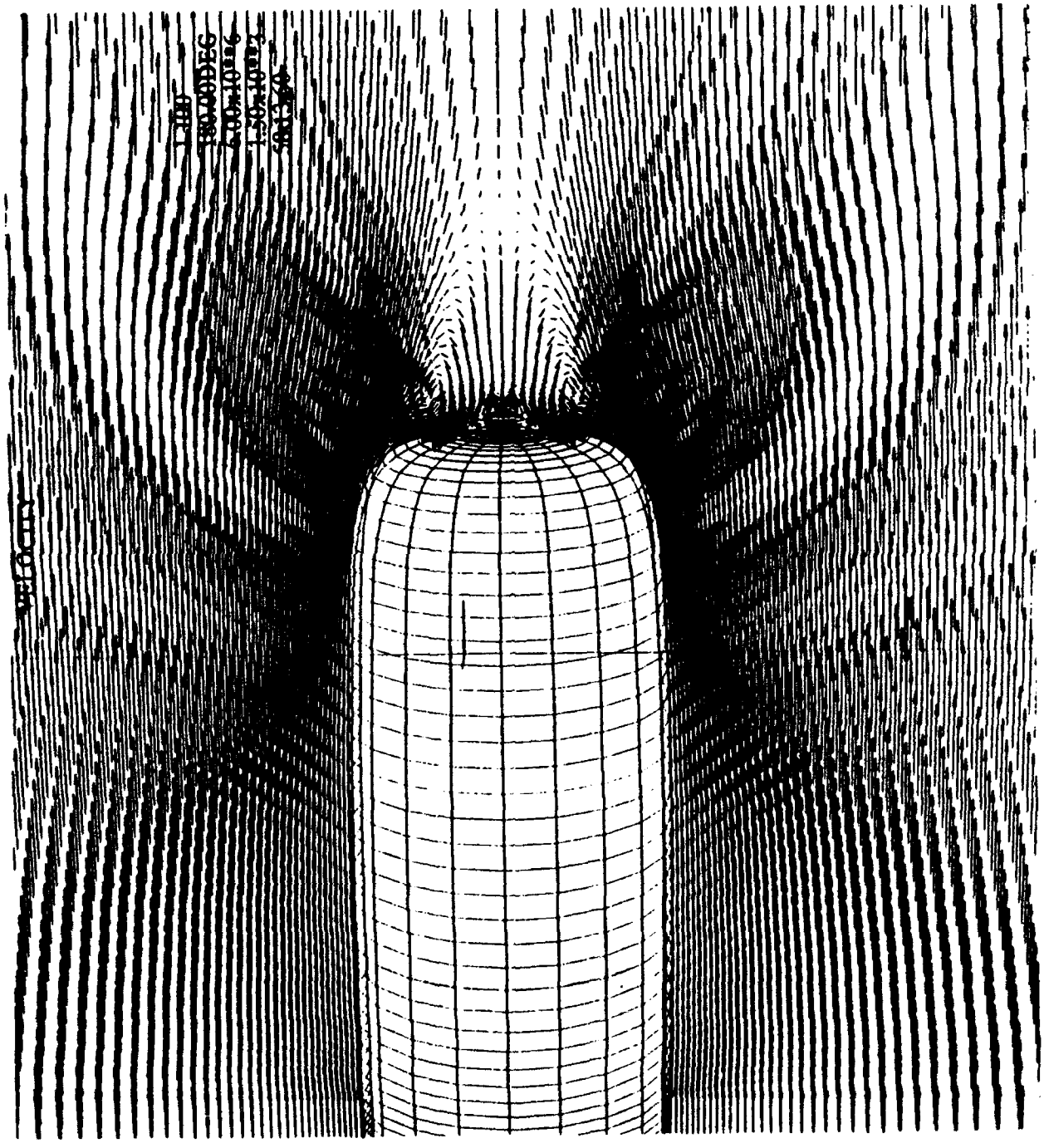

Figure 22. Velocity vectors for $M_\infty = 1.0$.

APPENDIX B
COMPUTER PROGRAMS

```
************************************************************************
*                                                                      *
*     This program is designed to calculate  KSI(X),                   *
*     K(X), and X using numerical integration based                    *
*     on trapezoidal rule to solve Eqn.(24) and                        *
*     plotting the output as  shown in Figs.1 & 3 .                    *
*                                                                      *
************************************************************************

      PROGRAM KSI
      REAL M(3),X(0:401,3),A,A1,B(401,3)
     +     ,KSI,P,FUNC,H,DD,Q,L,K(401,3),N,N1
      INTEGER YY
      OPEN(UNIT=9,FILE='KSI',STATUS='UNKNOWN')

      PRINT *,'ENTER LOWER & UPPER BOUND, # OF INTERVALS,
     +#OF DATA SET'
      READ *, A, A1, N, N1

100   DO 10 I=1,3
      PRINT *,'ENTER MACH NO. '
      READ *, M(I)
C      M(I) = 0.9+I*0.1

      IF (M(I).LT.1.0) THEN
      P=-1.
      ELSE
      P=1.
      ENDIF

      DO 20 J=1,N1
      B(J,I) = J*A1/N1
      H = (B(J,I)-A)/N
      AREA = 0.
      K(J,I)=(-0.0102/(M(I)**2))*((ABS((B(J,I)**2)-
     +((ABS(1-M(I)**2))**1.7574)))**(2./3.)+
     +(ABS(1-M(I)**2))**1.1716)

      DO 30 L=1 , N
      KSI = A + (L-0.5)*H
        DD = (KSI**2+P*(ABS(1-M(I)**2))**1.7574)
         IF (DD.GT.0.) THEN
         FUNC = 1./(DD**(1./3.))
         Q = 1.
         ELSE
```

```
            FUNC = 1./((-1*DD)**(1./3.))
            Q = -1.
            ENDIF
          AREA = AREA + H*FUNC*Q
          X(J,I) = AREA

   30     CONTINUE
   20     CONTINUE
   10     CONTINUE

          DO 40 J=1,N1
          PRINT 50, (B(J,I),X(J,I),K(J,I),I=1,3)
   50     FORMAT(1X,3(1F6.3,2F10.5,1X))
   40     CONTINUE

   200    PRINT*,'TRY AGAIN ? ENTER 1 FOR YES,2 FOR DATA
         +FILE,OTHERS FOR NO'
          READ *, YY
          IF (YY.EQ.1) THEN
            GO TO 100
          ELSE
             IF (YY.EQ.2) THEN
                DO 110 J=1,N1
                WRITE (9,50) (B(J,I),X(J,I),K(J,I),I=1,3)
   110          CONTINUE
                GO TO 200
             ENDIF
          ENDIF
          END
```

```
**********************************************************************
*                                                                    *
*      This program is written to calculate  ZETA(r) and             *
*      r using Eqn.(25) and plotting the output in Fig.3 .            *
*                                                                    *
**********************************************************************


      program zeta
      real M(3),zeta(0:14,3),r(14)
      open(unit=9,file='zz',status='unknown')

      do 10 I=1,3
c      M(I)=0.7+I*0.1
      print *, 'enter mach no.'
      read *, M(I)

      do 20 J=1,14
      zeta(0,I)=1000
      print *,'enter r values'
      read *, r(J)
c      r(J)=0.1*J
      zeta(J,I)=(4/(r(J)**2))+ (abs(1-(M(I)**2))*
     +(r(J)**2.8284))+((1-(M(I)**2))**2)*(r(J)**7.657)/50.63
      if (zeta(J,I).GE.zeta(J-1,I)) zeta(J,I)=zeta(J-1,I)
20    continue
10    continue

      print 30, M
30    format(11x,5F10.4)

      do 40 J=1,14
c      print 50, r(J),(zeta(J,I),I=1,4)
      write (9,50)  (r(J),zeta(J,I),I=1,3)
50    format (4x,3(2F10.4,2x))
40    continue
      end
```

```
*****************************************************************
*                                                               *
*     This program is written to calculate  Z(r) and  r         *
*     using Eqn.(59) and showing the output in Fig.4 .          *
*                                                              *
*****************************************************************


      PROGRAM  ZR
      REAL M(4),R(1000),Z(0:1000,4)
      OPEN(UNIT=99,FILE='ZR1',STATUS='UNKNOWN')

      DO 10 I=1,4
C      M(I) = 0.7 + I*0.1
      PRINT *, 'ENTER MACH NO. '
      READ *, M(I)

      DO 20 J=1,1000
      Z(0,I) = 0.0
      R(J) = 0.001*J
            Z ( J , I )    =    ( R ( J ) * * 3 ) / ( 8    -
(2.8284*(R(J)**4.8284)*ABS(1-(M(I)**2)))-
     +(0.1512*(R(J)**9.657)*((1-M(I)**2)**2)))
      IF (Z(J,I).LE.0.0)  Z(J,I)=Z(J-1,I)
20    CONTINUE
10    CONTINUE


      DO 40 J=1,1000
C      PRINT 50, R(J) , (Z(J,I),I=1,4)
      WRITE (99,50) R(J), (Z(J,I), I=1,4)
50    FORMAT(4X,5F10.6)
40    CONTINUE
      END
```

```
************************************************************************
*                                                                      *
*     This program is written to determine Rmin for                    *
*     transonic Mach numbers using Eqn.(60) and the                    *
*     output is shown in Fig.5 .                                       *
*                                                                      *
************************************************************************


      PROGRAM RMIN
      REAL M,R
      OPEN(UNIT=88,FILE='RMIN',STATUS='unknown')

      DO 100 M = 0.8,1.2,0.0001
      IF(M.LT.1.0)  THEN
         R=1.2074/((1-M**2)**0.2071)
      ELSE
         IF(M.GT.1.0)  THEN
           R=1.2074/((M**2-1)**0.2071)
         ELSE
           R = 7.0
         ENDIF
      ENDIF
C      PRINT 80, M,R
      WRITE (88,80) M,R
80    FORMAT(1X,F7.5,7X,1F10.6)
100   CONTINUE
      END
```

```
*****************************************************************
*                                                               *
*     This program is designed to numerically integrate         *
*     Z(r) ,Eqn.(64), based on trapezoidal rule .               *
*                                                               *
*****************************************************************


      PROGRAM  IZR
      REAL M(3),R(401,3),A,A1,IZ(0:401,3),H,FUNC,N,N1,Ro
      INTEGER YY
      OPEN(UNIT=55,FILE='IZR',STATUS='UNKNOWN')

100   DO 10 I=1,3
C      M(I) = 0.7 + I*0.1
      PRINT *, 'ENTER  MACH  NO. '
      READ *, M(I)
      PRINT *, 'DETERMINE THE VALUES OF MACH #',M(I)
      PRINT *, 'ENTER Rmin  ,A'
      READ *, A
      PRINT *, 'ENTER THE UPPER LIMIT OF R ,A1'
      READ *, A1
      PRINT *, 'ENTER # OF INTERVALS , N'
      READ *,N
      PRINT *, 'HOW MANY DATA SET DERIVED ? N1'
      READ *, N1
      PRINT *, 'INPUT Ro FOR THIS MACH # , Ro'
      READ *, Ro

      DO 20 J=1,N1
      R(J,I) = J*A1/N1
      H = (R(J,I)-A)/N
      AREA = 0.

      DO 30 L=1,N
      RR = A+(L-0.5)*H
      FUNC=(RR**3)/(8-(2.8284*(RR**4.8284)*ABS(1-(M(I)**2)))
     + -(0.1512*(RR**9.657)*((1-M(I)**2.)**2.)))
      AREA = AREA + H*FUNC
      IZ(J,I) = Ro - AREA

30    CONTINUE
20    CONTINUE
10    CONTINUE

      DO 40 J=1,N1
C      PRINT 50, (R(J,I),IZ(J,I),I=1,3)
```

```
      WRITE(55,50) (R(J,I),IZ(J,I),I=1,3)
50    FORMAT (1X,3(F6.3,F9.6,3X))
40    CONTINUE

      PRINT *,'TRY AGAIN ? ENTER 1 FOR #YES#, OTHERS FOR #NO#'
      READ *, YY
      IF (YY.EQ.1) GO TO 100
      END
```

```
*****************************************************************
*                                                               *
*     This program is using numerical integration to            *
*     determine the supersonic boundary surfaces ,              *
*     Eqn.(64), and calculating pressure coefficient            *
*     and local Mach number profiles, using Eqns.(40            *
*     & 49). The output is shown in Figs.(6-13) .               *
*                                                               *
*****************************************************************

      PROGRAM CPP
      REAL X(401,9),Y(401,6), XR(401),YR(401),M,MX,XYMAT
      INTEGER I,J,K,L,IWRITE

      OPEN(UNIT=52,FILE='cp15.dat',STATUS='UNKNOWN')
      OPEN(UNIT=53,FILE='cp11.dat',STATUS='UNKNOWN')
      OPEN(UNIT=54,FILE='cp12.dat',STATUS='UNKNOWN')
      OPEN(UNIT=77,FILE='cpp.dat',STATUS='UNKNOWN')
      OPEN(UNIT=78,FILE='m105.dat',STATUS='UNKNOWN')
      OPEN(UNIT=79,FILE='tire1.dat',STATUS='UNKNOWN')
      OPEN(UNIT=80,FILE='tire2.dat',STATUS='UNKNOWN')

100   OPEN(UNIT=1,FILE='KSI.DAT',STATUS='OLD')
      OPEN(UNIT=2,FILE='IZR.DAT',STATUS='OLD')
      REWIND(UNIT=1)
      REWIND(UNIT=2)
      IWRITE =78
      MACP=52

        READ (1,*,END=50) ((X(I,J),J=1,9),I=1,401)
50      READ (2,*,END=60) ((Y(K,L),L=1,6),K=1,401)
60    DO 10 J=2,6,2

      PRINT *,' Ro is rmin ; EPSILON  is the accuracy '
      PRINT *,'ENTER  MACH  NO., Ro , EPSILON'
      READ  *, M,RO,EPS
      WRITE (77,*) M,RO,EPS
      XM = 1-M**2
      L = J/2*3

      DO 30 I = 1,401
      DO 20 K = 1,401
        IF(Y(I,J).LT.0.001) THEN
          GO TO 10
        ELSE
          XYMAT = ABS(Y(I,J)-ABS(X(K,L)))
          IF(XYMAT.GT.EPS) THEN
            GO TO 20
            ELSE
```

```
            XR(K) = X(K,L-1)/RO
            YR(I) = Y(I,J-1)/RO
            ZETA = (4./(Y(I,J-1)**2)) + ABS(XM)*Y(I,J-1)**2.8284
     +           + XM**2*(Y(I,J-1)**7.657)/50.63
            Cp = (-2/(M**2*2.4))*(0.2208*ZETA*(X(K,L-2)**2 +
     +          (ABS(XM))**1.7574)**(1./3.)+XM)
            MX = SQRT(ABS((M**2*(1-Cp)/(1+0.2*M**2*Cp))))
C            PRINT 90, X(K,L-1),Y(I,J-1),Cp,MX
            WRITE(77,40) X(K,L-1),Y(I,J-1),Cp,MX
            WRITE(MACP,40) XR(K) ,YR(I) ,Cp ,MX
            WRITE(IWRITE,70) XR(K) , YR(I)
            GO TO 30
          ENDIF
        ENDIF

20      CONTINUE
30      CONTINUE
        IWRITE=IWRITE+1
        MACP =MACP+1
10      CONTINUE

40      FORMAT (1X,4(F15.7,2X))
70      FORMAT (1X,2F17.9)
90      FORMAT (1X,4(F15.7,2X))

        PRINT *,'TRY AGAIN ? 1 FOR YES!,2 FOR NO!!'
        READ *, IY
        IF(IY.EQ.1) GO TO 100
        END
```

```
*****************************************************************
*                                                               *
*     This program is written to determine the sonic            *
*     boundary  surface M = 1.0, ro = 4.0 using Eqn.(78),       *
*     and calculating pressure  coefficient and local           *
*     Mach profile using Eqns.(79 & 80). The output is          *
*     shown in Figs. 16 & 17 . Some output files are used       *
*     in CFD.                                                   *
*                                                               *
*****************************************************************


      program sonic
      real M(0:160),r(0:160),x(0:160),zeta(0:160),ksi(0:160),
     +     z(0:160),k(0:160),Cp(0:160), RR(0:160),YY(0:160),
     +     xx(0:160),xxx(0:160)

      open(unit=11,file='sonic1.dat',status='unknown')
      open(unit=22,file='sonic2.dat',status='unknown')
      open(unit=33,file='sonic3.dat',status='unknown')
      open(unit=66,file='sonic4.dat',status='unknown')

c     sonic1.dat  => x , r , Cp , M
c     sonic2.dat  => x , r  (horintal)
c     sonic3.dat  => x , r  (vertical)
c     sonic4.dat  => x/ro , r/ro , Cp , M

      do 10 I = 0, 159
      x(I) = I*0.1
      ro = 4.0
      r(I) = (abs(ro**4. - 0.004*(x(I)**4.)))**0.25
      RR(I) = r(I)/ro
      YY(I) = - 1.0* RR(I)
      xx(I) = x(I)/ro
      xxx(I) = 3.975 - xx(I)
      zeta(I) = 4./(r(I)**2.)
      ksi(I) = (x(I)**3.)/27.0
      z(I) = r(I)**3.
      k(I) = - 0.00101*(x(I)**4.)
      Cp(I) = - 0.1840 * zeta(I)*(ksi(I)**0.6667)
      M(I) = (abs((1-Cp(I))/(1 + 0.2*Cp(I))))**0.50
c      print *, xx(I) ,RR(I) ,Cp(I) ,M(I)
10    continue

      do 20 I =0, 159
      write(11,50) xx(I) , rr(I) , Cp(I) , M(I)
      write(22,60) xxx(I) , RR(I) , YY(I)
      write(33,70) xxx(I),YY(I)
```

```
      write(66,50) x(I) ,r(I) ,Cp(I) ,M(I)
50    format(2x,1f8.4,2x,3f14.7,2x)
60    format(2x,1f8.3,2x,2f12.6,2x)
70    format(10x,1f12.6,5x,f12.6)
20    continue

      write(34,80)(xxx(I),i=0,159,3)
      write(34,80)(xxx(i),i=156,0,-3)
      write(34,80)(yy(i),i=0,159,3)
      write(34,80)(rr(i),i=156,0,-3)
80    format(5(1x,f12.6,',',))

      do 30 I =158, 0 ,-1
      write(33,70) xxx(I),RR(I)
30    continue
      end
```

INITIAL DISTRIBUTION LIST

		No. Copies
1.	Defense Technical Information Center Cameron Station Alexandria VA 22304-6145	2
2.	Library, Code 052 Naval Postgraduate School Monterey CA 93943-5002	2
3.	Chairman Department of Aeronautics, Code AA/Co Naval Postgraduate school Monterey, CA 93943-5000	1
4.	Prof. Oscar Biblarz Department of Aeronautics, Code AA/Bi Naval Postgraduate school Monterey, CA 93943-5000	3
5.	Prof. Garth Hobson Department of Aeronautics, Code AA/Hg Naval Postgraduate school Monterey, CA 93943-5000	1
6.	Mr. Ed. Gravelin Nasp Jpo WPAFB Dayton, OH 45433	1
7.	Dr. Craig Porter Naval Weapons Center, Code 3591 China Lake, CA 93555	1
8.	Mr. James 1. Hunt Ms 350 Langley Res. Center Hampton, VA 23665-5225	1
9.	1st. Lt. Waleed I. Al-hashel P.O. Box # 20114 Manama Bahrain	3